Accepted Manuscript

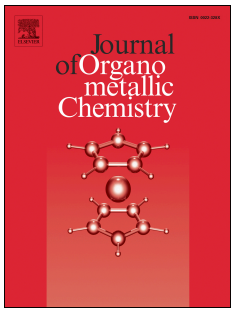

Synthesis and Molecular Structure of Ruthenium(III) Benzoylhydrazone Complexes: Substituents Effect on Transfer Hydrogenation of Ketones

Appukutti Kanchana Devi, Rengan Ramesh, Nattamai Bhuvanesh

PII: S0022-328X(15)00244-2

DOI: 10.1016/j.jorganchem.2015.04.032

Reference: JOM 19018

To appear in: *Journal of Organometallic Chemistry*

Received Date: 30 January 2015

Revised Date: 10 April 2015

Accepted Date: 15 April 2015

Please cite this article as: A. Kanchana Devi, R. Ramesh, N. Bhuvanesh, Synthesis and Molecular Structure of Ruthenium(III) Benzoylhydrazone Complexes: Substituents Effect on Transfer Hydrogenation of Ketones, *Journal of Organometallic Chemistry* (2015), doi: 10.1016/j.jorganchem.2015.04.032.

Air stable paramagnetic Ru(III) complex bearing a benzoylhydrazone ligand incorporating $PPh_3$and chloride as co-ligands. The molecular structures of two of the complexes were confirmed by single crystal X-ray diffraction analysis. The catalytic efficiency of the complex is investigated for different ketonessuch as aromatic/heterocyclic/cyclic and aliphatic ketones in the presence of base with in 5 h. The effect of other variables on the transfer hydrogenation reaction, such as solvent, base, temperature, time, catalyst screening and catalyst loadingon the catalytic activity of the complexes is also investigated

Graphical abstract

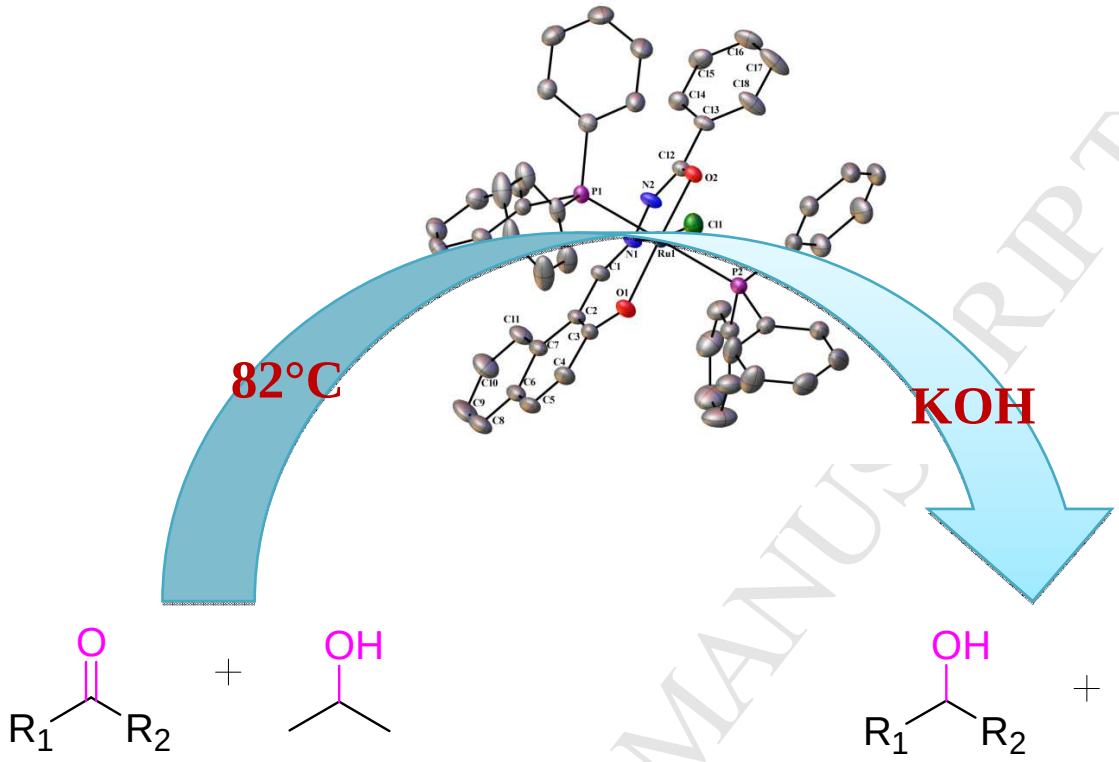

Conversion is up to 99%

ABSTRACT

An easy and convenient synthesis of a new series of octahedral ruthenium(III) complexes bearing benzoylhydrazone of general formula $[Ru(L)Cl(PPh_3)_2]$ (where L = 2-hydroxy-1-naphthaldehyde benzoylhydrazone) has been reported. The composition of all the complexes has been unequivocally characterized by microanalysis, IR, electronic, magnetic and EPR spectroscopic techniques. The substituted benzoylhydrazone ligands behave as a dianionic tridentate O, N and O donors and coordinate to ruthenium *via* the phenolic oxygen, the azomethine nitrogen and the deprotonated amide oxygen. The complexes exhibit moderately strong ligand-to-metal charge transfer transitions in the visible region and intraligand transition in the UV region. Magnetic moment of the complexes (298 K) lies in the range 1.72-1.97 μB reveals the presence of one unpaired electron in the metal center. The low spin mononuclear Ru(III) benzoylhydrazone complexes display rhombic EPR spectral pattern in frozen solution. The molecular structure of two of the complexes has been established by single crystal X-ray crystallography and indicates the presence of a distorted octahedral geometry in these complexes. Further, the complexes **1-5** have been proven to catalyse the transfer hydrogenation of linear, cyclic and aromatic ketones to their corresponding secondary alcohols in the presence of *i*-PrOH/KOH at 82 °C and the maximum conversion is up to 99%. The effect of other variables on the transfer hydrogenation reaction such as solvent, base, temperature, time and catalyst loading is also reported.

Key words: Benzoyl hydrazone, Ru(III) complex, Synthesis, Characterization, X-ray structure, Transfer hydrogenation.

Synthesis and Molecular Structure of Ruthenium(III) Benzoylhydrazone Complexes: Substituents Effect on Transfer Hydrogenation of Ketones

Appukutti Kanchana Devi [a], Rengan Ramesh [a,*] and Nattamai Bhuvanesh[b]

[a]*School of Chemistry, Bharathidasan University, Tiruchirappalli-620024, India.*

[b]*Department of Chemistry, Texas A&M University, USA*

**To whom correspondence should be made: +91-431-2407053, Fax: +91-431-2407045,*

INTRODUCTION

Generally, the coordination chemistry of hydrazone based ligands proved to be very interesting, because of their excellent complexation ability towards transition metals and the possibility of analytical applications. Hydrazones, produced from the reaction of hydrazides with aldehydes or ketones, have very active sites for transition-metal atoms to coordinate with C=N and C=O groups. The chemical interest arises from the ability of benzoylhydrazone to adopt various coordination modes, leading to enormous structural diversity of their complexes. They can easily be modified by variation of the parent aldehydes or ketones used for their synthesis. These chelating ligands can exhibit amido-imidol tautomerism (Scheme 1) and coordinate in either neutral [1], monoanionic [2], dianionic [3-5] or tetraanionic [6] form bearing unusal coordination numbers, such as six and seven [3, 7] in some mono or binuclear species. However, coordination modes are depended on the reaction conditions, such as metal ion, its concentration, the pH of the medium and the nature of the hydrazone ligand [2].The most predominant coordination mode is bidentate, achieved through hydrazine nitrogen and carbonyl oxygen atoms [8]. When a third donor site (D) is incorporated into the ligands, D, N, O- tricoordination also takes place. Though several hydrazone metal complexes are known for their biological activities [9], catalytic applications of these complexes are not much studied [10, 11].

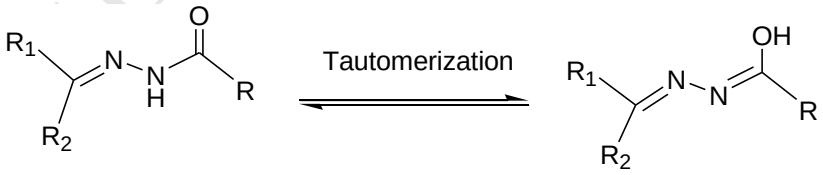

Scheme 1. Amide and imidol forms of hydrazone

The reduction of C=O and C=N bonds forming alcohols and amines, respectively, is among the most fundamental molecular transformations. The development of new and effective catalytic systems for transfer hydrogenation reaction by simple solvent as the proton

source like 2-proponal, formaldehyde etc., continues to be the focus of many efforts designed to develop new technologies for future industrial applications [12-14]. Organic synthesis needs economically and technically more benign methods that are very general. From an industrial point of view, catalytic transfer hydrogenation is an alternative source for high-pressure catalytic hydrogenation with molecular hydrogen [15]. 2-proponal is the conventional source having favourable properties; it is stable, operational simplicity (b.p. 82 °C), nontoxic, environmentally and economically favoured and then dissolves many organic compounds [16]. The acetone by-product is readily removable [17]. The most active systems are based on Ru, Rh and Ir containing nitrogen, oxygen-and/or phosphorous bearing ligands, which lead to the easy formation of catalytically active intermediate species. Catalytic hydrogenation using a phosphine in conjugation with an appropriate metal, usually ruthenium is a versatile method which requires only very low levels of catalyst. Numerous ruthenium(II) complexes have been reported as catalyst precursors for the transfer hydrogenation of ketones and have shown high activity [18-23]. The most outstanding results have been obtained by Noyori's group who discovered and developed the catalyst [$RuCl_2$(diphosphine)(diamine)] with >99% yield [24]. W. Du group reported highly active Ru(II) complex catalysts bearing bis(trifluoromethyl)pyrazolyl−pyridyl-based NNN ligands for the transfer hydrogenation of ketones with high TOF [25]. As recently demonstrated by Pavel A. Duband co-workers, exhibited a high activity [RuX_2(diphosphine)(1,2-diamine)] system showing excellent selectivity and reactivity for reduction of acetophenone derivatives [26]. Robert H. Morris and co-workers described the complexes of the type *trans*- RuHCl(diphosphinite)(diamine) and their application in the asymmetric transfer hydrogenation of ketones with 99% conversion [27].

Compared with ruthenium(II) analogues, there exist relatively few reports on

paramagnetic ruthenium(III) complexes containing tertiaryphosphine/arsine and chlorides and their catalytic applications to transfer hydrogenation [28-30]. Low-spin ruthenium(III) complexes containing diphenylphosphanyl imidazole (**1a**) has been proved to be an efficient pre-catalyst for transfer hydrogenation of ketones without any mechanism [31]. Further, Zhengkun Yu et al reported Ru(III) complexes bearing a tridentate dimethylpyrazol and its derivatives (**1b**) as efficient catalysts for transfer hydrogenation reaction [32]. In addition, (pyridyl)benzoazole ruthenium(III) complexes (**1c**) were reported as catalysts for transfer hydrogenation of ketones by Ojwach et al [33].

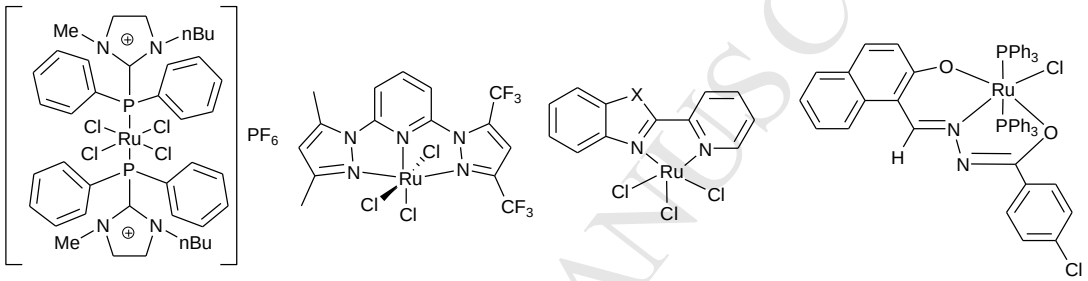

1a **1b** **1c** **1d**

In view of the growing interest on the catalytic activities of ruthenium complexes in the transfer hydrogenation of ketones, in the present report, we have described the synthesis and characterization of a series of mononuclear Ru(III) complexes with the tridentate 2-hydroxy-1-napthaldehyde benzoylhydrazone along with triphenylphosphine and chloride as ancillary ligands (**1d**). The composition of the complexes was accomplished by analytical and spectral methods. The molecular structure of the two of the complexes **1** and **3** has been determined by X-ray crystallography. Further, the catalytic efficiency of the complexes has been explored for the transfer hydrogenation of a wide range of ketones.

RESULTS AND DISCUSSION

Synthesis of the Complexes

A new series of mononuclear ruthenium(III) benzoylhydrazone complexes of the

type [Ru(L)(Cl)(PPh_3)$_2$] was achieved by reacting ruthenium(III) precursors [$RuCl_3(PPh_3)_3$] with the tridentate benzoylhydrazone ligand (L_1-L_5) in 1:1 molar ratio in the presence of catalytic quantity of triethylamine. The addition of triethylamine to the reaction mixture was used to abstract a proton from the imidol oxygen and to facilitate the coordination of the imidolate oxygen to the ruthenium(III) ion. The synthesized ruthenium(III) benzoylhydrazone complexes are stable in air at room temperature, non-hygroscopic in nature and highly soluble in common organic solvents such as dichloromethane, chloroform, acetonitrile, THF, etc., producing intense colour in their solution.

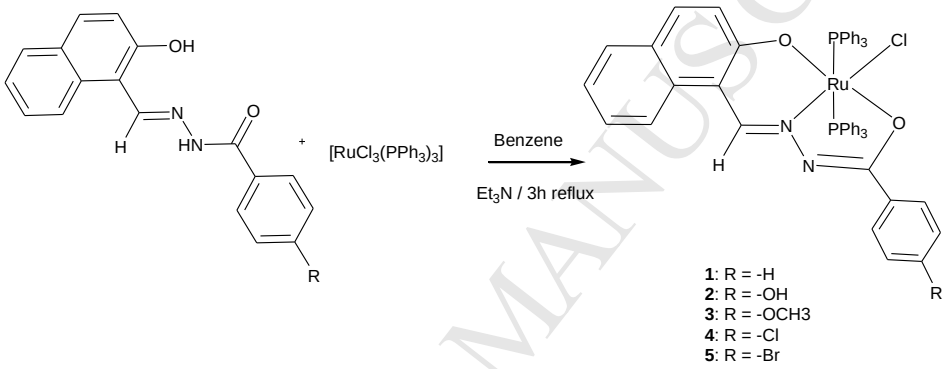

Scheme 2. Synthesis of ruthenium(III) complexes

Characterization of the Complexes

The free ligands showed a strong band in the regions 3370-3470 cm^{-1} and 3107-3222 cm^{-1} which are characteristic of the -OH and –NH functional groups respectively. The free ligands also display $\upsilon_{C=N}$ and $\upsilon_{C=O}$ absorptions in the region 1592-1697 cm^{-1}. The disappearance of strong band due to υ_{O-H} in all the complexes indicates the deprotonation of phenolic oxygen prior to coordination to the Ru(III) ion. The bands due to υ_{N-H} and $\upsilon_{C=O}$ stretching vibrations are also not observed in the complexes indicating that the ligand undergo tautomerization and subsequent coordination of the imidazole oxygen to the Ru(III) ion. This is also supported by the appearance of new bands in the region 1197-1252 cm^{-1} and 1564-1667 cm^{-1} which may be attributed to the C-O and -C=N-N=C- group respectively of

the coordinated ligand [34]. A sharp band near 330 cm^{-1} has been observed for all the complexes due to υ_{Ru-Cl} stretching frequency. In addition, other characteristic bands due to ruthenium bound triphenylphosphine in the region 1472-1556 cm^{-1} are also present in the spectra of all the complexes [35]. The IR spectral data of all the complexes confirm the coordination of the benzoylhydrazone ligand to ruthenium(III) ion *via* phenolate oxygen, the azomethine nitrogen and the imidolate oxygen.

The UV-Vis spectra of all the Ru(III) complexes were obtained in CH_2Cl_2 in the 200-800 nm range at ambient temperature. All the new complexes display three absorption bands in the ultraviolet and visible region. The moderately intense absorption band in the region 471–467 nm is probably due to charge transfer transitions taking place from the highest occupied ruthenium t_2g orbital (HOMO) to the vacant π^* orbital of the ligand (LUMO). Another intense absorption in the higher energy region (273–226 nm) may be attributed to usual $n \rightarrow \pi^*$, $\pi \rightarrow \pi^*$ transitions occurring within the ligand orbitals. The pattern of the electronic spectra of all the complexes indicate the presence of an octahedral environment around ruthenium(III) ion similar to that of other reported ruthenium(III) octahedral complexes [36].

The room temperature magnetic moment of the ruthenium(III) complexes (1-5) in the powder state are in the range 1.72-1.97 μ_B. The value indicates the presence of one unpaired electron, confirming a low spin t_{2g}^5 configuration and a +3 oxidation state for ruthenium in all the complexes [37, 38]. The electron paramagnetic resonance spectral studies are performed both in pure powder samples and in solution at room temperature and liquid nitrogen temperature respectively at X-band frequency. All the complexes exhibit well defined single isotropic feature near g = 2.02 to 2.23 at room temperature. However, the EPR spectral profiles of the complexes in dichloromethane solution at 77K show rhombic spectra with three different 'g' values ($g_x \neq g_y \neq g_z$) (**Fig**. S8, Supporting Information). Each complexes

display three distinct signals indicating the distortion of the NO_2ClP_2 coordination sphere around the metal centre from octahedral geometry. Overall the position of lines and nature of the EPR spectra of the complexes are characteristic of low spin ruthenium(III) octahedral complexes [39, 40].

X-ray Crystallographic Studies.The molecular structure of the complexes **1** and **3** has been determined by single crystal X-ray crystallography in order to determine the solid state structural parameters. The ORTEP diagram of **1** and **3** are illustrated in Figs. 1 and 2 respectively. The summary of crystal data, data collection and refinement parameters are given in Table 1. The bond parameters associated with the metal centre are listed in Table 2. The benzoylhydrazone ligand coordinates meridionally to the ruthenium(III) ion in a tridentate manner *via* the phenolate oxygen, the azomethine nitrogen and the deprotonated amide oxygen in the benzoylhydrazone fragment forming one five membered and one six membered chelate rings. The complex (**1**) crystallizes in the '$P12_1/n1$' space group. The coordinated benzoylhydrazone ligand and chloride ligand constitute one equatorial plane with the metal at the centre. Further, the chloride ligand is *trans* to the azomethine nitrogen. The two triphenylphosphine ligands are mutually *trans* to each other. Ruthenium(III) ion is therefore sitting in a NO_2ClP_2 coordination environment and adopts a distorted octahedral geometry as reflect in all the bond parameters around ruthenium(III) ion. The bond angles around ruthenium(III) ion are O(1)-Ru(1)-P(1) = 91.43(5)°, O(2)-Ru(1)-P(1)=93.70°, O(1)-Ru(1)-P(2) = 87.87(5)°, O(2)-Ru(1)-P(2) =87.56(4)°, N(1)-Ru(1)-Cl(1)= 171.40(5)° and bond lengths of 1.9906(15) Å for Ru(1)-O(1), 2.0382(14)Å for Ru(1)-O(2), 2.0011(18)Å for Ru(1)-N(1), 2.3686(7)Å for Ru(1)-Cl(1), 2.4021(7)Å for Ru(1)-P(1), 2.4071(7)Å for Ru(1)-P(2) [41]. Further, the structure of the complex (**3**) adopts similar structure as in the complex (**1**) with slight changes in bond angles and bond distances. As all the complexes display

similar spectral properties, the other three complexes are assumed to have similar structure to that of complexes (**1**) and (**3**). The X-ray determinations confirm the structure proposed on the basis of spectroscopic data, consistent with metal trivalency and the diionized nature of the ligands.

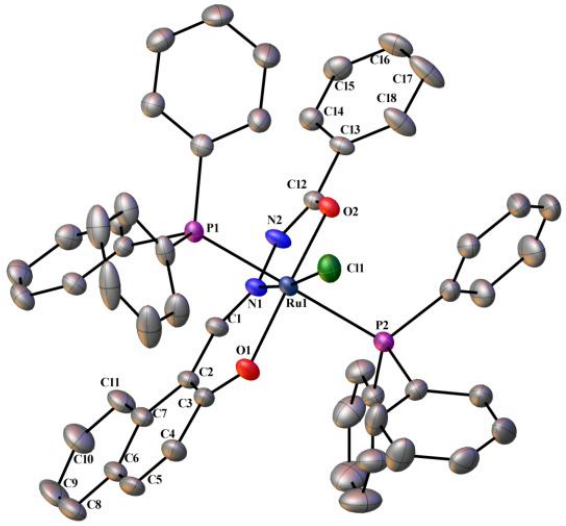

Fig. 1. ORTEP diagram of the complex (**1**), hydrogen atoms have been omitted for clarity

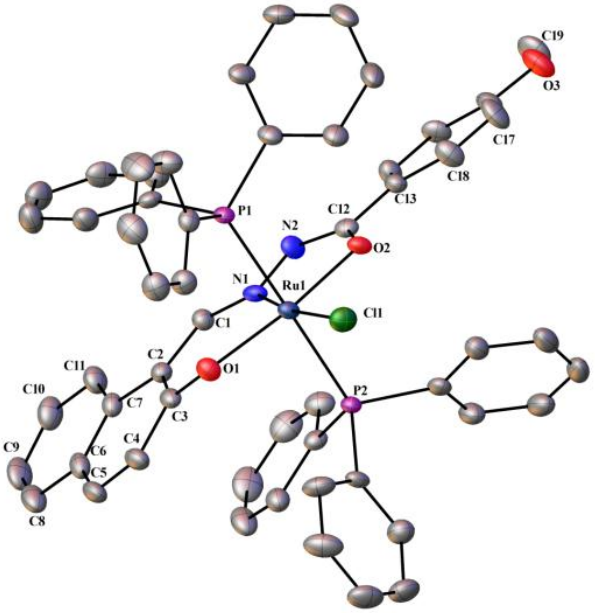

Fig. 2. ORTEP diagram of the complex (**3**), hydrogen atoms have been omitted for clarity.

193 **Table 1**

194 Crystal data and structure refinement for complexes (**1**) and (**3**)

	Complex 1	**Complex 3**
Empirical formula	$C_{54}H_{42}ClN_2O_2P_2Ru$	$C_{55}H_{44}ClN_2O_3P_2Ru$
Formula weight	949.35	979.38
Temperature (K)	150.15	150.15
Wavelength (Å)	0.71073	0.71073
Crystal system	Monoclinic	Monoclinic
Space group	$P12_1/n1$	$P12_11$
a (Å)	12.493(3)	11.668(2)
b (Å)	18.761(4)	16.610(3)
c (Å)	19.725(4)	12.540(2)
α (°)	90	90
β (°)	103.211(2)	111.081(2)
γ (°)	90	90
Crystal size(mm^3)	0.21x0.2x0.05	0.32x0.18x0.1
Volume ($Å^3$)	4500.9(16)	2267.8(8)
Z	4	2
D_{calcd} (Mg/m^3)	1.401	1.434
Absorption coefficient	0.523 (mm^{-1})	0.523 (mm^{-1})
F(000)	1948	1006
Theta range for data collection (°)	1.517 to 27.461	1.740 to 27.558
Limiting indices	-16<=h<=16, -24<=k<=24, -25<=l<=25	-14<=h<=14, -21<=k<=21, -14<=l<=16
Completeness to theta=25.242°	99.9%	99.7%
Absorption correction	Semi-empirical from equivalents	Semi-empirical from equivalents
Reflection collected	42033	20443
Refinement method	Full-matrix least-squares on F^2	Full-matrix least-squares on F^2
Data/restraints/parameters	10218 / 0 / 559	10110 / 1 / 579
Goodness-of-fit on F^2	1.064	1.065
Final R indices [I >2σ(I)]	R_1 = 0.0345, wR_2 = 0.0755	R_1 = 0.0351, wR_2 = 0.0708
R indices (all data)	R_1 = 0.0485, wR_2 = 0.0833	R_1 = 0.0465, wR_2 = 0.0774
Largest diff. peak & hole	0.469 and -0.534 e. $Å^{-3}$	0.670 and -0.413 e. $Å^{-3}$

195

Table 2

Selected bond lengths (Å) and angles (°) for the complexes (**1**) & (**3**)

Complex	1	3
Ru(1)-Cl(1)	2.3686(7)	2.3567(13)
Ru(1)-P(1)	2.4021(7)	2.4088(11)
Ru(1)-P(2)	2.4071(7)	2.3990(11)
Ru(1)-O(1)	1.9906(15)	1.996(3)
Ru(1)-O(2)	2.0382(14)	2.026(3)
Ru(1)-N(1)	2.0011(18)	1.991(4)
O(1)-C(3)	1.328(3)	1.324(5)
O(2)-C(12)	1.299(2)	1.291(5)
N(1)-N(2)	1.403(2)	1.398(5)
N(1)-C(1)	1.298(3)	1.295(6)
N(2)-C(12)	1.306(3)	1.311(6)
Cl(1)-Ru(1)-P(1)	88.47(2)	90.56(5)
Cl(1)-Ru(1)-P(2)	89.08(2)	91.34(5)
O(1)-Ru(1)-P(1)	91.43(5)	88.90(9)
O(1)-Ru(1)-P(2)	87.87(5)	90.71(9)
O(2)-Ru(1)-P(1)	93.70(5)	89.37(9)
O(2)-Ru(1)-P(2)	87.56(4)	90.61(9)
N(1)-Ru(1)-O(2)	77.89(6)	78.39(13)
N(1)-Ru(1)-Cl(1)	171.40(5)	170.91(12)
N(1)-Ru(1)-P(1)	89.15(5)	89.99(11)
N(1)-Ru(1)-P(2)	93.43(5)	88.15(11)

Catalytic transfer hydrogenation of ketones

The transfer hydrogenation reactions involving transfer of hydrogen from one organic substrate to another are of great importance in organic synthesis, since one can avoid the use of molecular hydrogen. We have performed the transfer hydrogenation of various ketones using all Ru(III) hydrazone complexes as catalysts. The necessity of the ruthenium complex to observe the ensuing transfer hydrogenation was ascertained by carrying out a

series of blank or control experiments which suggest that none of $RuCl_3.3H_2O$ or benzoylhydrazone ligand or as a mixture causes the transformations under identical conditions. In a typical experiment, acetophenone (0.2 mmol), ruthenium(III) complex (1 mol %) and KOH (0.08 mmol) in 6 ml of isopropanol were taken into the round bottom flask and are heated to reflux for 5 h at 82 °C. The catalyst was removed from the reaction mixture by the addition of diethyl ether followed by filtration and subsequent neutralization with 1 M HCl. The organic layer was filtered through the short path of silica gel by column chromatography and is subjected to GC analysis. The catalyst performed efficiently in the conversion of acetophenone to 1-phenyl ethanol. In order to optimize the reaction conditions for better results, the effect of different solvents, bases, temperature, time and catalyst: substrate (C:S) ratio was studied.

To study the influence of solvents in our catalytic system, we have chosen the reaction between acetophenone (0.2 mmol), complex 4 (1 mol %) as the catalyst precursor in the presence of various solvents and KOH as the base and the results are listed in Table 3. Methanol, ethanol and isopropanol solvents were taken for investigation and isopropanol is found to be a suitable system for the maximum conversion (99%) of acetophenone to 1-phenylethanol. On the other hand ethanol solvent gave less conversion (47%) than isopropanol. The lowest conversion (12%) was obtained with methanol solvent. Based on this conclusion 2-propanol was taken as a proton source for our investigation.

Table 3

Effect of the solvent and base[a]

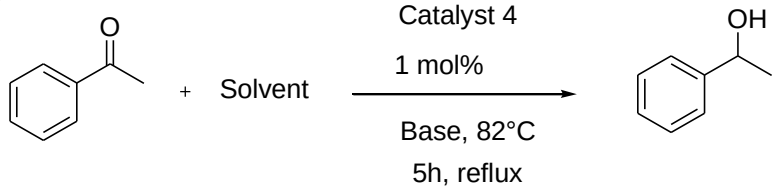

Entry	Solvent	Base	Conversion [b] (%)
1	Methanol	KOH	47
2	Ethanol	KOH	12
3	*Iso*-propanol	KOH	100
4	*Iso*-propanol	---	0
5	*Iso*-propanol	KOH	0 [c]
6	*Iso*-propanol	NaOH	99
7	*Iso*-propanol	$NaHCO_3$	51
8	*Iso*-propanol	Na_2CO_3	68
9	*Iso*-propanol	K_2CO_3	72
10	*Iso*-propanol	Et_3N	Trace
11	*Iso*-propanol	Pyridine	Trace

[a] Experimental conditions: reactions were carried out using acetophenone (0.2 mmol), catalyst (1 mol %), base (0.08 mmol), *iso*-propanol (6 ml) at 82 °C for 5h.

[b] Conversion was monitored by GC analysis and are average of two runs.

[C] Reaction carried out in the absence of catalyst.

In order to improve the catalytic transfer hydrogenation, we examined the influence of different bases. We initially carried out the reaction of acetophenone (0.2 mmol), using complex **4** (1 mol %) as a test catalyst in the presence of isopropanol with different bases. The strong inorganic bases like NaOH or KOH gave higher conversion of 99% and 100% respectively. Whereas, weak inorganic bases such as Na_2CO_3 and K_2CO_3 shows moderate conversion of 79% and 82% respectively. Organic bases such as triethylamine, pyridine we observed only traces amount of alcohol was formed. The conversions are summarized in Table 3. The results indicate that the conversion was strongly dependent upon the base strength with the stronger bases giving the higher conversion.

Acetophenone has been chosen as a model substrate to explore the catalytic activity of the complexes **1-5** under the optimized conditions. The reduction of acetophenone (0.2 mmol) to 1-phenyl ethanol by 2-propanol in the presence of KOH base has been to

inspect the catalytic behaviour of the complexes **1-5** (1 mol %) in transfer hydrogenation. All the complexes efficiently catalyze the transfer hydrogenation of acetophenone with maximum conversion within 5 h. Among the tested complexes, complex **4** is highly efficient in the transfer hydrogenation of ketones to alcohol with a high conversion of 100%. The result of transformations is given in Table 4. So, we decided to further explore its catalytic activity in the reduction of ketones. Complexes containing chloro and bromo substituents show effective conversions 100% and 98% respectively. The introduction of electron withdrawing groups such as -Cl or -Br on the complexes shows high conversion in comparison with electron releasing group. It was observed that the presence of electron withdrawing group on the aromatic ring possibly decreased the electron density on the metal center and hence the rate of transfer hydrogenation increases. The lowest conversion observed is 79% for complex **2**. The catalytic process is more efficient with the complex **4** followed by **5**, **1**, **3** and complex **2** showing the least activity among all five complexes.

Table 4

Transfer hydrogenation of acetophenone to 1-phenylethanol catalyzed by complexes (**1-5**)[a]

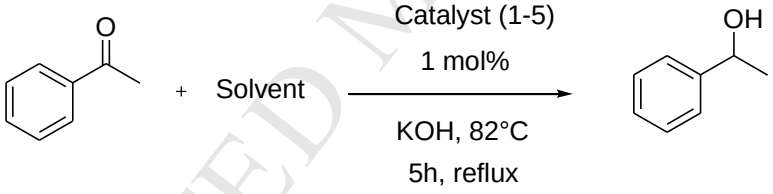

Entry	Complex	Conversion[b] (%)
1	**1**	85
2	**2**	79
3	**3**	82
4	**4**	100
5	**5**	98

[a] Experimental conditions: reactions were carried out at 82 °C using acetophenone (0.2 mmol), catalyst (1 mol %), base (0.08 mmol) and *iso*-propanol (6 mL).

[b] Conversion was monitored by GC analysis and are average of two runs.

Low catalyst loading tests were competent to discover the effectiveness of the catalyst. The designing of a new catalyst in a catalytic system is either to enhance the rate of

regeneration, to slow down the rate of decomposition of catalyst or to decreases the quantity of catalyst used. Hence, the ability to use small amounts of catalyst and still achieve high conversions is a great concern in transfer hydrogenation reactions due to the high cost of metals and ligands used. In the course of our studies into developing efficient formation of alcohol, we became interested to find the varying the catalyst/substrate ratio. In order to optimize the effect of catalyst loading, different catalyst: substrate (C:S) ratios were tested in the transfer hydrogenation reaction of acetophenone using complex **4** as catalyst in *i*-PrOH/KOH. The reaction proceeds with high conversion (95%) when the catalyst loading is 0.2 mol %. When decreasing the catalyst loading to 0.15, 0.1 mol %, the reaction proceeds with good conversions 76% and 70% respectively. Further, the catalyst works well with low loading of catalyst 0.06 mol % and shows conversion of 60%. Thus it was concluded that the catalyst loading of 0.2 mol % of Ru catalyst is the best compromise between optimum reaction rate. The results are collected in Table 5 and the conversions reported are averages of two runs in the case of all catalytic reaction.

Table 5

The effect of low loading catalyst on transfer hydrogenation reaction[a]

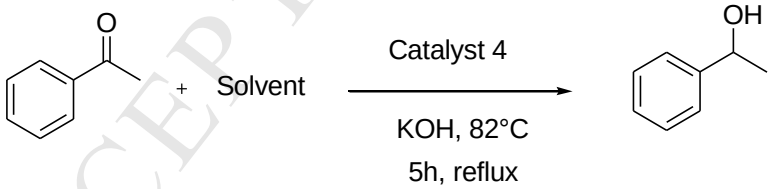

Entry	Mol % Ru	Conversion[b] (%)	TON[c]
1	1.0	100	99
2	0.3	97	290
3	0.2	95	477
4	0.15	76	533
5	0.1	70	705
6	0.06	60	898

[a] Experimental conditions: reactions were carried out at 82 °C using acetophenone (0.2 mmol), catalyst (0.06 –1 mol %), base (0.08 mmol), *iso*-propanol (6 ml).

[b] Conversion was monitored by GC analysis and are average of two runs.

[C] TON = Turnover number = ratio of moles of product formed to moles of catalyst used.

The progress of formation of 1-phenylethanol as a function of time using the above optimized conditions is depicted in Fig. 3. The results indicate the formation of 1-phenylethanol initially increased with the progress of the reaction, reached a maximum and then remain unchanged. A high conversion (95%) for the formation of 1-phenylethanol was observed at the optimum reaction time of 5 h. No noticeable improvement was observed even after extending the reaction time to 7 h.

The results obtained from the optimization studies indicate clearly that excellent conversion was achieved in the reduction of acetophenone to 1-phenylethanol when **4** was used as the catalytic precursor with 0.2 mol % catalyst in 2-propanol, containing KOH as a base, refluxed for 5 h at 82 °C.

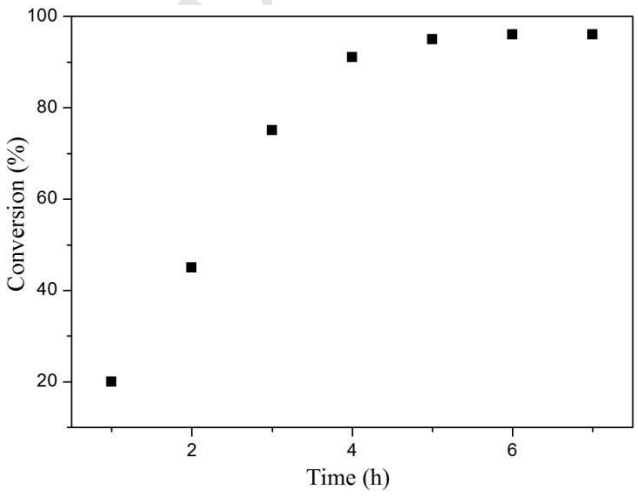

Fig. 3. Influence of reaction time on the formation of 1-phenylethanol

To examine the generality of complex **4** as a catalyst for transfer hydrogenation, the scope of ketones with different electronic effect was investigated under similar conditions

and several representative results are summarized in Table 6. The complex exhibits impressive efficiency towards the transfer hydrogenation of substituted ketones. Acetophenone with substituents of varying electronic properties were efficiently reduced to the corresponding secondary alcohols in excellent conversions. The conversion of acetophenone to 1-phenyl ethanol is obtained in 95% conversion (entry 1). The presence of electron-withdrawing or electron-donating substituents on the aromatic ring has significant effect in the conversion. Aromatic halo substituents have an enhancing effect on the catalytic activity, showing quantitative results on the formation of the corresponding alcohols (entries 2, 3 and 4) and catalyzed with excellent conversions of 97%, 98% and 99% respectively when compared to that of acetophenone. Whereas, electron donating substituents (4'-methyl, 4'-methoxy and 4'- hydroxyl acetophenone) on the ring gave lower conversions to the corresponding alcohols are 91%, 89% and 75% (entries 5, 6 and 7) respectively than that of acetophenone. The introduction of electron withdrawing substituents to the para position of the aryl ring of the acetophenone decreased the electron density on the C=O bond. So, that the activity was improved giving rise to easier hydrogenation. Thus electron-withdrawing groups on acetophenone benefit the catalytic activity while electron donating group decrease it. Order of the reactivity of substituted acetophenone is NO_2 > Br > Cl > H > Me > OMe > OH. Further, sterically hindered ketone benzophenone (entry 8) underwent hydrogenation to give the corresponding secondary alcohol in moderate conversion of 84%. The scope the present catalyst is further explored to heterocyclic ketones and are less common. Interestingly, heterocyclic aromatic ketone such as 2-acetylthiophene and 2-acetylpyridine (entries 9 and 10) shows the conversion of 82% and 93% respectively. Moreover this catalyst shows efficient activity for the transfer hydrogenation of five to seven membered cyclic ketones i.e., cyclopentanol results 89%, cyclohexanol 78% and cyclohepatanol 66% conversion (entries 11, 12 and 13). The complex efficiently catalyse the reduction of aliphatic

335 ketones such as ethyl methyl ketone, methyl propyl ketone and isobutyl methyl ketone to
336 their corresponding alcohols with 95%, 88% and 82% respectively (**Figs**. S28-S43,
337 Supporting Information).

338 **Table 6**

339 Transfer hydrogenation of various ketones with complex (**4**)[a]

340 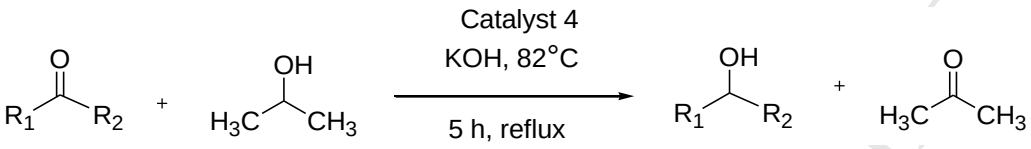

Entry	Substrate	Product	Conversion[b] (%)	TON[c]
1	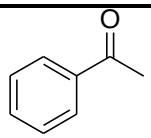	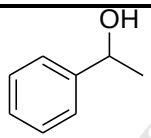	95	477
2	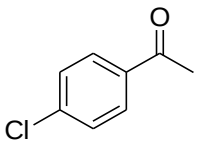	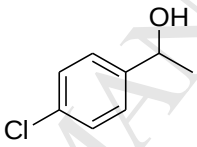	97	485
3	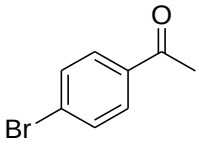	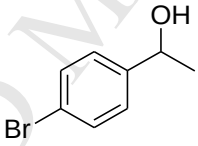	98	492
4	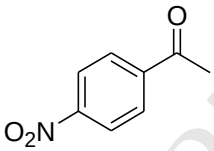	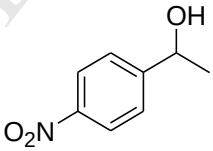	99	496
5	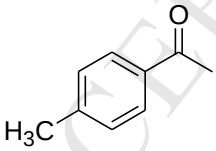	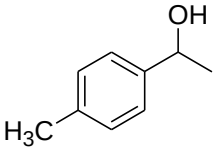	91	455
6	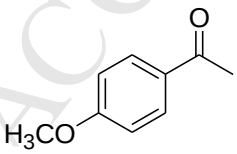	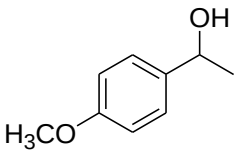	89	447
7	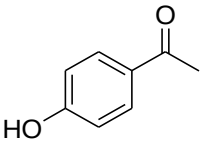	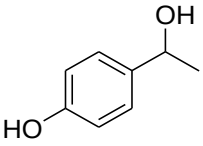	75	378

8	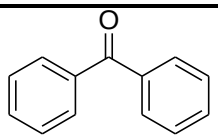	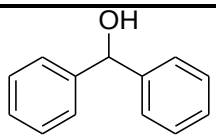	84	422
9	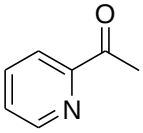	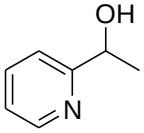	93	463
10	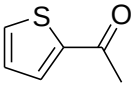	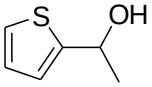	82	412
11	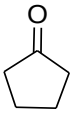	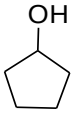	89	447
12	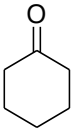	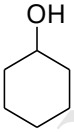	78	390
13	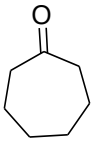	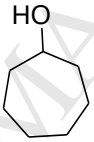	66	330
14	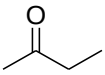	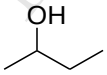	95	474
15	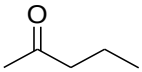	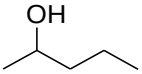	88	439
16	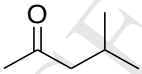	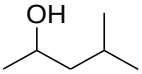	82	413

[a] Experimental conditions: reactions were carried out at 82 °C using ketone (0.2 mmol), catalyst (0.2 mol%), base (0.08 mmol), *iso*-propanol (6 ml).

[b] Conversion was monitored by GC analysis and are average of two runs.

[C] TON = Turnover number = ratio of moles of product formed to moles of catalyst used.

It is well known from the literature that the mechanism of transfer hydrogenation of ketones by ruthenium complexes has been proposed to involve the formation of

ruthenium(II)-hydride as catalytic intermediate [42] and the mechanism involving Ru(III) complexes is not known. However, the present Ru(III) complexes show excellent catalytic performance with high conversions and the reasons are not clear. Further, it is believed that the transfer hydrogenation may be associated with the reduction of Ru(III) to Ru(II) [33]. We are currently investigating the scope and mechanism of these catalysts. The catalytic activity of the present complexes is more efficient than the reported octahedral ruthenium complexes in terms of conversion, reaction time and catalyst loading [43, 44].

Conclusions

The present work reports the synthesis of five ruthenium(III) complexes containing benzoylhydrazone ligands. Synthesized complexes were characterized by various analytical and spectroscopic techniques. All the complexes are one electron paramagnetic and display rhombic EPR spectra typical of d^5 low-spin metal centre. The molecular structure two of the complexes has been confirmed by X-ray structure determination which confirms the O,N,O coordination mode of hydrazones and reveals the presence of a distorted octahedral geometry around ruthenium ion. Further, all the Ru(III) benzoylhydrazone complexes were developed as effective and modular catalytic system for the transfer hydrogenation of a range of ketones. In addition, the influence of the substituent of the ligands and the substrates was studied and overall the catalytic rate increases with electron releasing substituents. The reported complexes work well with the low catalyst loading of 0.06 mol % and further studies on the mechanism of this interesting catalytic system are under progress.

EXPERIMENTAL SECTION

Materials

$RuCl_3.3H_2O$ was purchased from Loba-Chemie Pvt. Ltd., and was used as supplied.

Triphenylphosphine, 2-hydroxy-1-naphthaldehyde, benzhydrazide derivatives and the ketones used for catalysis were purchased from Sigma-Aldrich and were used as received. All the reagents used were chemically pure and analar grade. The solvents were freshly distilled prior to use following the standard procedures [45] and degassed before use. The precursor ruthenium(III) complex $[RuCl_3(PPh_3)_3]$ [46] was prepared by reported literature method. The substituted benzoyl hydrazone ligands were prepared by a reported literature method [47].

Physical measurements

Melting points were recorded in open capillaries with a Boetius micro-heating table and are uncorrected. The analysis of carbon, hydrogen and nitrogen were performed by analytical function testing Vario EL III CHNS elemental analyser at STIC, Cochin University of Science and Technology, Cochin, India. FT-IR spectra were recorded in KBr pellets with a JASCO 400 plus spectrometer in the range 4000-400 cm^{-1}. The electronic spectra were recorded, in dichloromethane, on a Cary 300 Bio UV–Vis Varian spectrophotometer in the range of 800-200 nm. The NMR spectra were recorded in DMSO-d^6 for the ligands with a Bruker 400 *MHz* instrument using TMS as the internal reference. EPR spectra of the powdered samples were recorded on a JEOL JES-FA200 EPR spectrometer instrument in X-band frequencies at RT and LNT, the field being calibrated with 2, 2-diphenyl-1-picrylhydrazyl. Diamagnetic corrections were estimated from Pascal constants [48] were used to obtain the molar paramagnetic susceptibilities. Organic compounds in catalysis were identified by gas chromatography (GC) using Bruker 436-GC using GC-FID detector equipped with a capillary column (15 m - 0.25 mm - 0.25 mm) and high purity nitrogen as carrier gas.

Preparation of benzoylhydrazone ligands

To a stirred ethanolic solution (10 mL) of 4-substituted benzhydrazides (0.86g,

5mmol), a solution of 2-hydroxy-1-naphtahldehyde (0.68-1 g, 5mmol) in ethanol (10 mL) was added dropwise. The reaction mixture was refluxed for 6 h, the solution concentrated to 5mL and cooled to room temperature. The solid formed was filtered, washed with cold methanol (5 mL) and dried in vaccum. The structures of the ligands were elucidated by elemental analysis, IR and ^{1}H NMR methods. The ^{1}H and ^{13}C NMR spectra for the ligands are exactly as would be expected (**Figs**. **S3-S7**, Supporting Information).

Synthesis of ruthenium(III) benzoylhydrazone complexes

All the [Ru(L)(Cl)(PPh_3)$_2$] complexes have been synthesized by a general procedure. Therefore the specific details are given below for a particular case. Solid [$RuCl_3(PPh_3)_3$] (50 mg, 0.05 mmol) was added to a benzene solution of L1-L5 (14.5-18.6 mg, 0.05 mmol) and $N(C_2H_5)_3$ (0.5 mL) as the base. The reaction mixture was refluxed for 3 h, when a brown colour solid was obtained. The reaction progress was monitored by using TLC. The brown colour solid precipitated was collected by filtration, washed with hexane and finally dried in air. Scheme 2 provides an overview of the complexes described in this work. The micro analytical data for the complexes are satisfactory with the proposed molecular formula.

Analytical and spectral data for the complexes

[Ru(L1)(Cl)(PPh_3)$_2$] (1): Colour: Brown; Yield: 83%; M.p.: 208-210 °C (with decomposition); Anal. Calc. for $C_{54}H_{42}ClN_2O_2P_2Ru$ (949.35 g mol^{-1}): C, 68.22%; H, 4.33%; N, 2.84%. Found: C, 68.31%; H, 4.46%; N, 2.95%. IR (KBr, cm^{-1}): 1197 $\upsilon_{(C-O)}$, 1583 $\upsilon_{(-C=N-N=C-)}$. UV-Vis (CH_2Cl_2, λ_{max}/nm; ε/dm^3 mol^{-1} cm^{-1}): 469(720), 270(5743), 227(8546). Magnetic susceptibility (μ_{eff}): 1.72BM. ESR (g_x, g_y, g_z) = 2.39, 2.22, 1.76.

[Ru(L2)(Cl)(PPh_3)$_2$] (2): Colour: Brown; Yield: 81%; M.p.: 231-233 °C (with decomposition); Anal. Calc. for $C_{54}H_{42}ClN_2O_3P_2Ru$ (965.14 g mol^{-1}): C, 67.26%; H, 4.46%; N, 2.81%. Found: C, 67.18%; H, 4.39%; N, 2.90%. IR (KBr, cm^{-1}): 1243 $\upsilon_{(C-O)}$, 1564 $\upsilon_{(-C=N-}$

$_{N=C-}$). UV-Vis (CH_2Cl_2, λ_{max}/nm; ε/dm^3 mol^{-1} cm^{-1}): 471(581), 273(4448), 226(6374). Magnetic susceptibility (μ_{eff}): 1.85BM. ESR (g_x, g_y, g_z) = 2.59, 2.34, 1.74.

[Ru(L3)(Cl)(PPh$_3$)$_2$] (3): Colour: Brown; Yield: 77%; M.p.: 245-247 °C (with decomposition); Anal. Calc. for $C_{55}H_{44}ClN_2O_3P_2Ru$ (979.15 g mol^{-1}): C, 67.32%; H, 4.41%; N, 2.72%. Found: C, 67.45%; H, 4.53; N, 2.86%. IR (KBr, cm^{-1}): 1212 $\upsilon_{(C-O)}$, 1597 $\upsilon_{(-C=N-N=C-)}$. UV-Vis (CH_2Cl_2, λ_{max}/nm; ε/dm^3 mol^{-1} cm^{-1}): 467(558), 271(4492), 227(8953). Magnetic susceptibility (μ_{eff}): 1.78BM. ESR (g_x, g_y, g_z) = 2.40, 2.11, 1.80.

Ru(L4)(Cl)(PPh$_3$)$_2$] (4): Colour: Brown; Yield: 86%; M.p.: 212-214 °C (with decomposition); Anal. Calc. for $C_{54}H_{41}Cl_2N_2O_2P_2Ru$ (983.10 g mol^{-1}): C, 65.86%; H, 4.12%; N, 2.93%. Found: C, 65.92%; H, 4.20; N, 2.85%. IR (KBr, cm^{-1}): 1252 $\upsilon_{(C-O)}$, 1634 $\upsilon_{(-C=N-N=C-)}$. UV-Vis (CH_2Cl_2, λ_{max}/nm; ε/dm^3 mol^{-1} cm^{-1}): 471(722), 273(4325), 228(6189). Magnetic susceptibility (μ_{eff}): 1.97BM. ESR (g_x, g_y, g_z) = 2.36, 2.09, 1.75.

Ru(L5)(Cl)(PPh$_3$)$_2$] (5): Colour: Brown; Yield: 89%; M.p.: 219-221 °C (with decomposition); Anal. Calc. for $C_{54}H_{41}BrClN_2O_2P_2Ru$ (1027.05 g mol^{-1}): C, 63.16%; H, 3.95%; N, 2.65%. Found: C, 63.07%; H, 4.02; N, 2.72%. IR (KBr, cm^{-1}): 1230 $\upsilon_{(C-O)}$, 1667 $\upsilon_{(-C=N-N=C-)}$. UV-Vis (CH_2Cl_2, λ_{max}/nm; ε/dm^3 mol^{-1} cm^{-1}): 471(603), 272(4460), 229(6292). Magnetic susceptibility (μ_{eff}): 1.89 BM. ESR (g_x, g_y, g_z) = 2.42, 2.22, 1.93.

X-ray crystallography

Single crystals of complexes **1** and **3** were grown by slow evaporation of their solution in dichloromethane-petroleum ether mixture. In each case, A BRUKER APEX 2 X-ray (three-circle) diffractometer was employed for crystal screening, unit cell determination, and data collection. The detector was set at 6.0 cm from the crystal sample (APEX2, 512x512 pixel). The X-ray radiation employed was generated from a Mo sealed X-ray tube (K_α =

0.70173Å with a potential of 40 kV and a current of 40 mA) fitted with a graphite monochromator in the parallel mode (175 mm collimator with 0.5 mm pinholes). Sixty data frames were taken at widths of 0.5°. These reflections were used in the auto-indexing procedure to determine the unit cell. A suitable cell was found and refined by nonlinear least squares and Bravais lattice procedures. Integrated intensity information for each reflection was obtained by reduction of the data frames with the program [49]. The integration method employed a three dimensional profiling algorithm and all data were corrected for Lorentz and polarization factors, as well as for crystal decay effects. The absorption correction program SADABS [50] was employed to correct the data for absorption. Hydrogen atoms were placed in idealized positions and were set riding on the respective parent atoms. All non-hydrogen atoms were refined with anisotropic thermal parameters. Absence of additional symmetry and voids were confirmed using PLATON. The structure was refined (weighted least squares refinement, XL [51] on F^2) to convergence [52]. Olex2 was employed for the final data presentation and structure plots.

Typical procedure for transfer hydrogenation of ketones

The mixture of a ketone (0.2 mmol) and base (0.08 mmol) containing the catalyst (0.002 mmol) in *i*-PrOH (6ml) was stirred at 82 °C. After the reaction was complete, diethyl ether could be added to the mixture and extract the ruthenium complexes followed by filtration and neutralized with 1 N HCl, washed with water and dried over anhydrous Na_2SO_4. Conversion obtained is related to the residual unreacted ketone. The alcohol products were identified by comparison with the authentic samples. Acetone was identified as only by-product in all the cases. As the catalyst is stable in all organic solvents and it can be recovered and the work up process is also very simple for this catalytic system.

ACKNOWLEDGEMENTS

One of the authors (A. K.) thank University Grants Commission (UGC), New Delhi, for the award of UGC-BSR RFSMS. We are thankful to the SERB-DST New Delhi for GC instrument facility through research project.

Appendix A. Supplementary material

^{1}H and ^{13}C-**N**MR spectra of ligands, UV-Vis and EPR spectra of representative complexes. CCDC 1023482, CCDC 1023481 contains the supplementary crystallographic data for complex **1** and **3**. These data can be obtained free of charge from The Cambridge Crystallographic Data Centre *via www.ccdc.cam.ac.uk/data_request/cif*. GC analysis data of reduced products.

REFERENCES

[1] S. Abram, C. Maichle-Mossmer, U. Abram, Polyhedron 17 (1998) 131-143.

[2] G.F. de Sousa, C.A.L. Filgueiras, A. Abras, S.S. Al-Juaid, P.B. Hitchcock, J.F. Nixon, Inorg. Chim. Acta. 218 (1994) 139-142.

[3] D. Wester, G.J. Palenik, Inorg. Chem. 15 (1976) 755-761.

[4] K. Andjelkovic, I. Ivanovic, S.R. Niketic, B. Prelesnik, V.M Leovac, Polyhedron 16 (1997) 4221-4228.

[5] K. And-jelkovic, G. Jakovljevic, M. Zlatovic, Z. Tesic, D. Sladic, J. Howing, R. Tellgren, J. Serb. Chem. Soc. 69 (2004) 651-660.

[6] A. Bonardi, C. Merlo, C. Pelizzi,G. Pelizzi, P. Tarasconi, F. Vitali, F.J. Cavatorta, Chem. Soc., Dalton Trans. 1991, 1063-1069.

[7] G.J. Palenik, D.W. Wester, Inorg. Chem. 17 (1978) 864-870.

[8] E.M.Y. Tido, E.J.M. Vertelman, A. Meetsma, P.J. Van Konigsbruggen, Inorg. Chim. Acta. 360 (2007) 3896-3902.

[9] (a) L. Sun, L. Hammarstrom, B. Akermark, S. Styring, Chem. Soc. Rev. 30 (2001) 36-49; (b) P.B. Sreeja, M.R.P. Karup, A. Kishore, C. Jasmine, Polyhedron 23 (2004) 575-581; (c) N. Chitrapriya, V. Mahalingam, L.C. Channels, M. Zeller, F.R. Fronczek, K. Natarajan, Inorg. Chim. Acta. 361 (2008) 2841-2850.

[10] For catalytic application of hydrazone complexes, See: R.N. Prabhu, R. Ramesh, RSC Adv. 2 (2012) 4515-4524.

[11] D. Pandiarajan, R. Ramesh, J. Organomet. Chem. 708 (2012) 18-24.

[12] R. Patchett, I. Magpantay, L. Saudan, C. Schotes, A. Mezzetti, F. Santoro, Angew.Chem., Int. Ed. 52 (2013) 10352-10355.

[13] W. Ye, M. Zhao, Z. Yu, Chem. Eur. J. 18 (2012) 10843-10846.

[14] M.T. Reetz, X. Li, J. Am. Chem. Soc. 128 (2006) 1044-1045.

[15] G. Zassinovich, G. Mestroni, S.Gladiali, Chem. Rev. 92 (1992) 1051-1069.

[16] J. Namy, J. Souppe, J. Collin, H.B. Kagan, J. Org. Chem. 49 (1984) 2045-2049.

[17] C.F. de Graauw, J.A. Peters, H. van Bekkum, J. Huskenes, Synthesis 1994, 1007-1017.

[18] (a) H.U. Blaser, C. Malan, B. Pugin, F. Spindler, H. Steiner, M. Studer, Adv. Synth. Catal. 345 (2003) 103-151.

[19] J. Hannedouche, G.J. Clarkson, M. Wills, J. Am. Chem. Soc. 126 (2004) 986-987.

[20] W. Baratta, P. Rigo, Eur. J. Inorg. Chem. 2008, 4041-4053.

[21] P. Sot, M. Kuzma, J. Vaclavik, J. Pechaacek, J. Prech, J. Januscak, P. Kacer, Organometallics 31 (2012) 6496-6499.

[22] R. Feng, A. Xiao, X. Zhang, Y. Tang, M. Lei, Dalton Trans. 42 (2013) 2130-2145.

[23] M. Babin, R. Clement, J. Gagnon, F.G. Fontaine, New J. Chem. 36 (2012) 1548-1551.

[24] H. Ohkuma, S. Ooka, T. Hashiguchi, Ikariya, R. Noyori, J. Am. Chem. Soc. 1995, 117, 2675-2676.

[25] W. Du, Q. Wang, L. Wang, Z. Yu, Organometallics 33 (2014) 974-982.

[26] A.D. Pavel, N.J. Henson, R.L. Martin, J.C. Gordon, J. Am. Chem. Soc. 136 (2014) 3505-3521.

[27] R. Guo, C. Elpelt, X. Chen, D. Song, R.H. Morris, Chem. Commun. 2005, 3050-3052.

[28] S. Kannan, K. Naresh kumar, R. Ramesh, Polyhedron 27 (2008) 701-708.

[29] G. Venkatachalam, R. Ramesh, Tetrahedron Lett. 46 (2005) 5215-5218.

[30] D. Pandiarajan, R. Ramesh, J. Organomet. Chem. 723 (2013) 26-35.

[31] C. Zhou, J. Zhang, M. Dakovic, Z. Popovic, X. Zhao, Y. Liu, Eur. J. Inorg. Chem. 2012, 3435-3440.

[32] W. Du, Q. Wang, L. Wang, Z. Yu, Organometallics 33 (2014) 974-982.

[33] A.O. Ogweno, S.O. Ojwach, M.P. Akerman, Dalton Trans. 43 (2014) 1228.

[34] R.N. Prabhu, R. Ramesh, RSC Advances 2 (2012) 4515-4524.

[35] G. Venkatachalam, R. Ramesh, S. Mobin, M. J. Organomet. Chem. 690 (2005) 3937-3945.

[36] G. Venkatachalam, R. Ramesh, Spectrochim. Acta A. 61 (2005) 2081-2087.

[37] R. Ramesh, Inorg. Chem. Commun. 7 (2004) 274-276.

[38] EPR studies of Ru(III) complexes, See: Y. Tanabe, S. Sugano, J. Phys. Soc. Japan. 9 (1954) 766-779.

[39] F.A. Cotton, M. Matusz, R.C. Torralba, Inorg. Chem. 28 (1989) 1516-1520.

[40] O.K. Medhi, U. Agarwala, Inorg. Chem. 19 (1980) 1381-1384.

[41] R. Raveendran, S. Pal, Inorg. Chim. Acta. 359 (2006) 3212-3220.

[42] For mechanism of transfer hydrogenation, See: J.E. Backvall, J. Organomet. Chem. 652 (2002) 105-111.

[43] B. J. Sarmah, D. K. Dutta, J. Organomet. Chem. 695 (2010) 781-785.

[44] M. U. Raja, E. Sindhuja, R. Ramesh, Inorg. Chem. Commun. 13 (2010) 1321–1324.

[45] W.L.F. Armarego, C.L.L. Chai, Purification of Laboratory Chemicals, sixth ed. Butterworth-Heinemann, Oxford, UK, 2009, pp 69-79.

[46] Experimental procedure for the Ru(III) starting precursor, See: J. Chatt, G.J. Leigh, D.M.P Mingos, R.J. Paske, J. Chem. Soc. A. 1968, 2636-2641.

[47] R.N. Prabhu, R. Ramesh, J. Organomet. Chem. 718 (2012) 43-51.

[48] W.E. Hatfield, Theory and Applications of Molecular Paramagnetism, Wiley, New York, 1976. p. 491.

[49] SADABS, G.M. Sheldrick, "Program for Absorption Correction of Area Detector Frames", BRUKER AXS Inc., 5465 East Cheryl Parkway, Madison, WI 53711-5373,USA.

[50] APEX2 "Program for Data Collection on Area Detectors" BRUKER AXS Inc., 5465 East Cheryl Parkway, Madison, WI 53711-5373 USA.

[51] G.M. Sheldrick, (2008). Acta Cryst. A64, 112-122. XS, XL, XT, BRUKER AXS Inc., 5465 East Cheryl Parkway, Madison, WI 53711-5373 USA.

[52] O.V. Dolomanov, L.J. Bourhis, R.J. Gildea, J.A.K. Howard, H. Puschmann, "OLEX2: A Complete Structure Solution, Refinement and Analysis Program", J. Appl. Cryst. 42 (2009) 339-341.

Research High Lights

- Five new Ru(III) benzoylhydrazone complexes were synthesized and characterized.
- Single crystal XRD confirms the octahedral geometry of the complexes.
- All the Ru(III) complexes were developed as catalyst for TH of ketones.
- Catalyst works well with 0.2 mol % and the conversion is up to 99%.

Supporting Information

For

Synthesis and Molecular Structure of Ruthenium(III) Benzoylhydrazone Complexes: Substituents Effect on Transfer Hydrogenation of Ketones

Appukutti Kanchanadevi [a], Rengan Ramesh [a,*] and Nattamai Bhuvanesh [b]

[a]*School of Chemistry, Bharathidasan University, Tiruchirappalli 620024, India.*

[b]*Department of Chemistry, Texas A&M University, USA.*

**To whom correspondence should be made: +91-431-2407053, Fax: +91-431-2407045, E-mail: ramesh_bdu@yahoo.com*

List of itmes

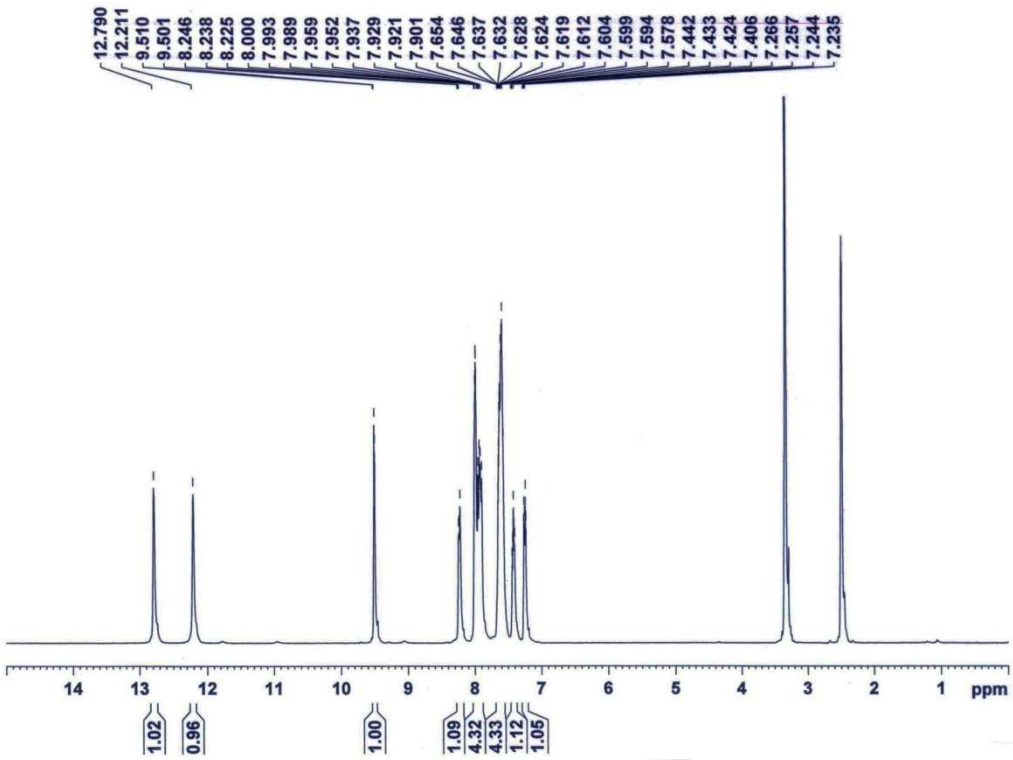

Figure S1: ^{1}H NMR for L_1

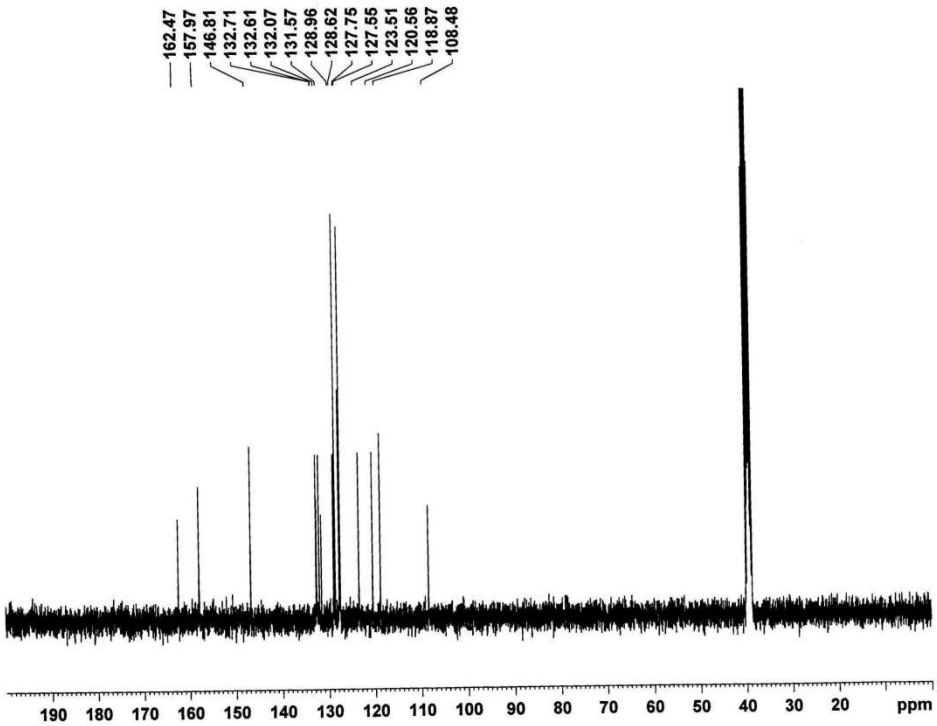

Figure S2: ^{13}C NMR for L_1

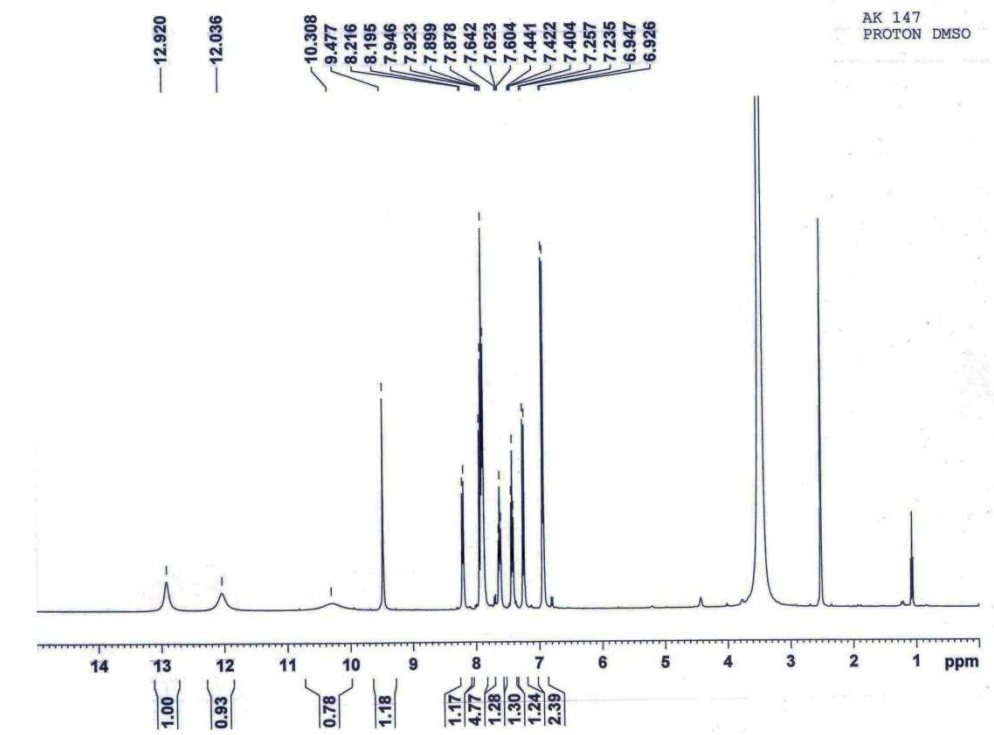

Figure S3: ^{1}H NMR for L_2

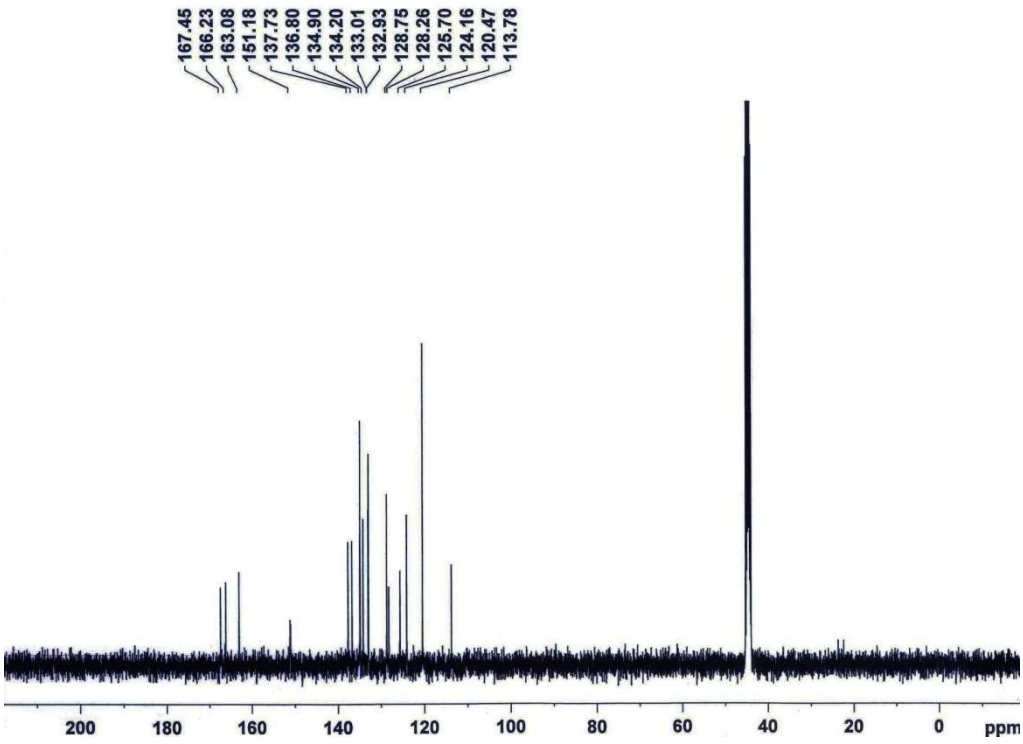

Figure S4: ^{13}C NMR for L_2

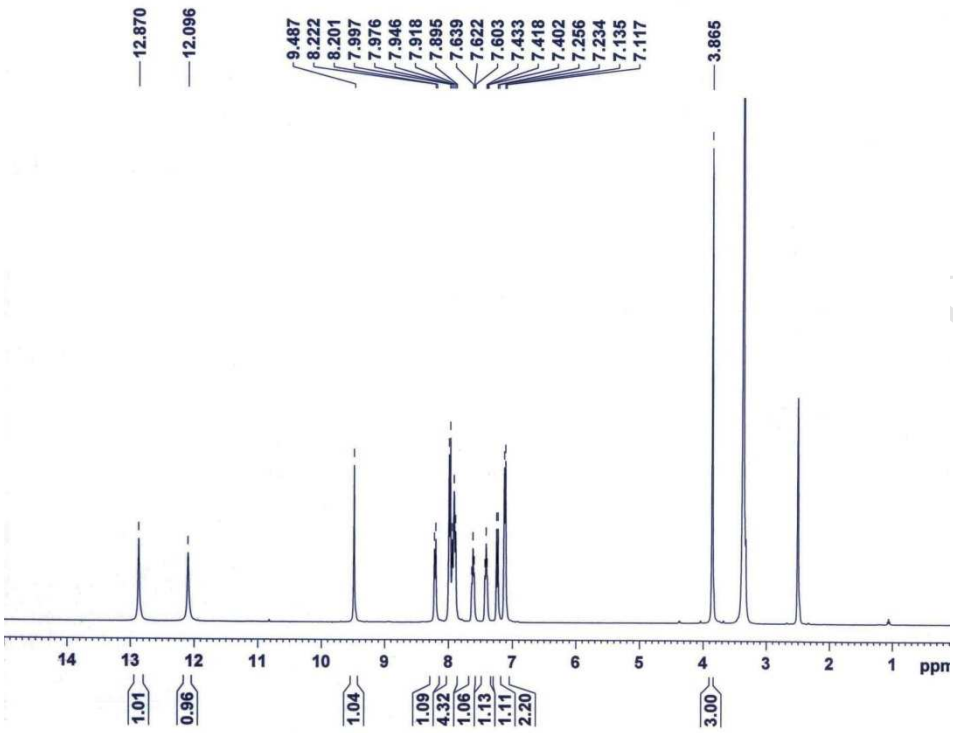

Figure S5: ^{1}H NMR for L_3

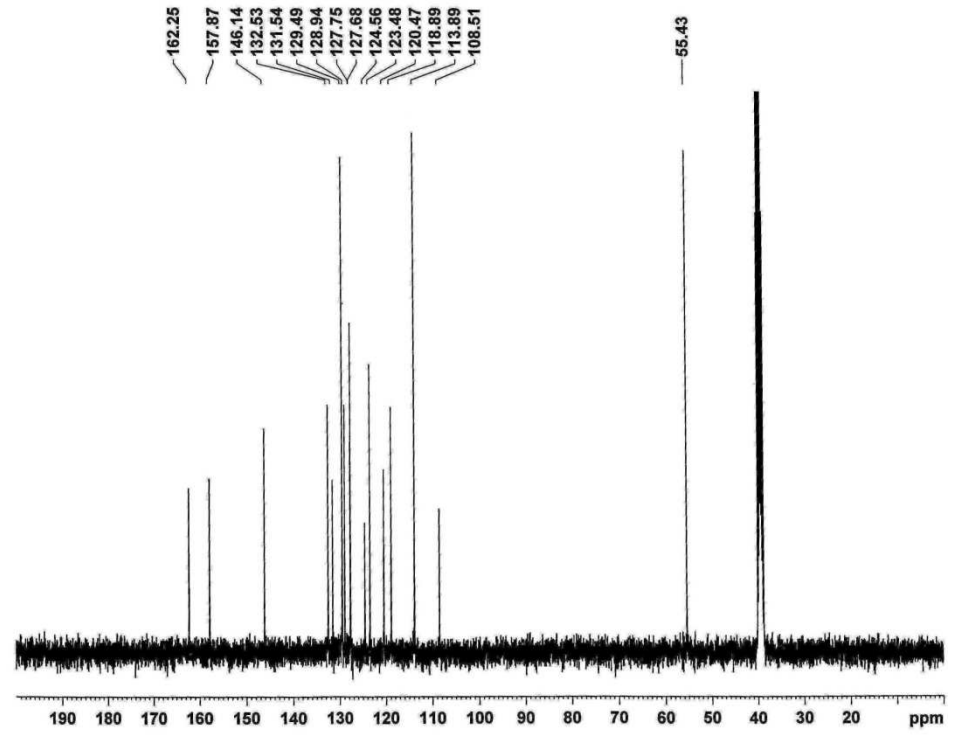

Figure S6: ^{13}C NMR for L_3

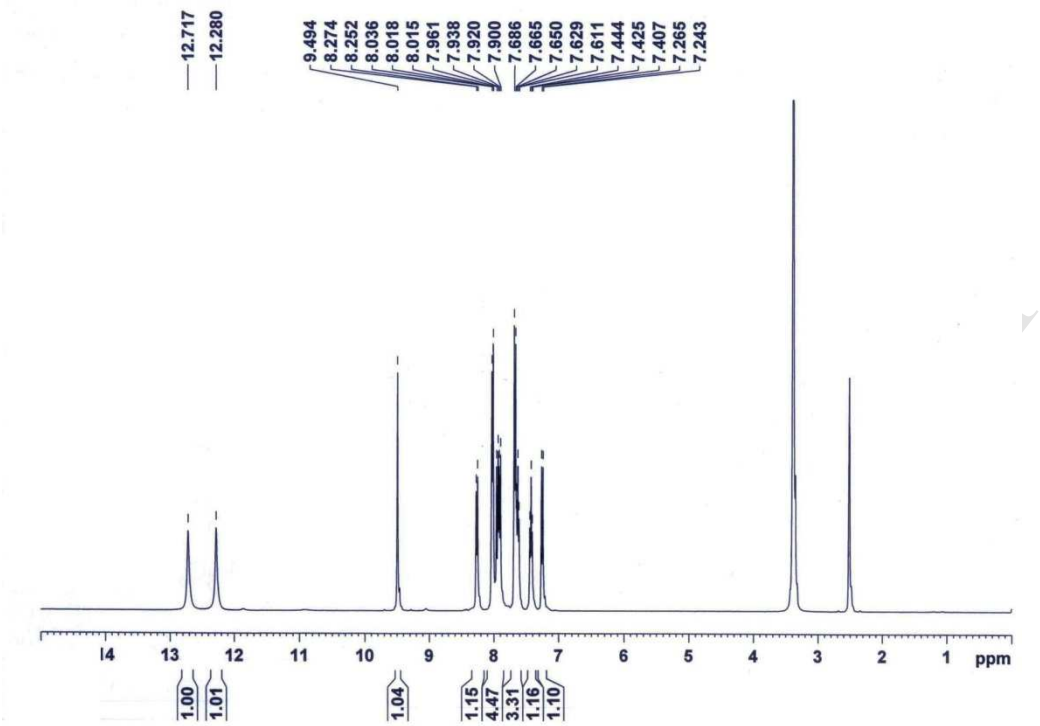

Figure S7: ^{1}H NMR for L_4

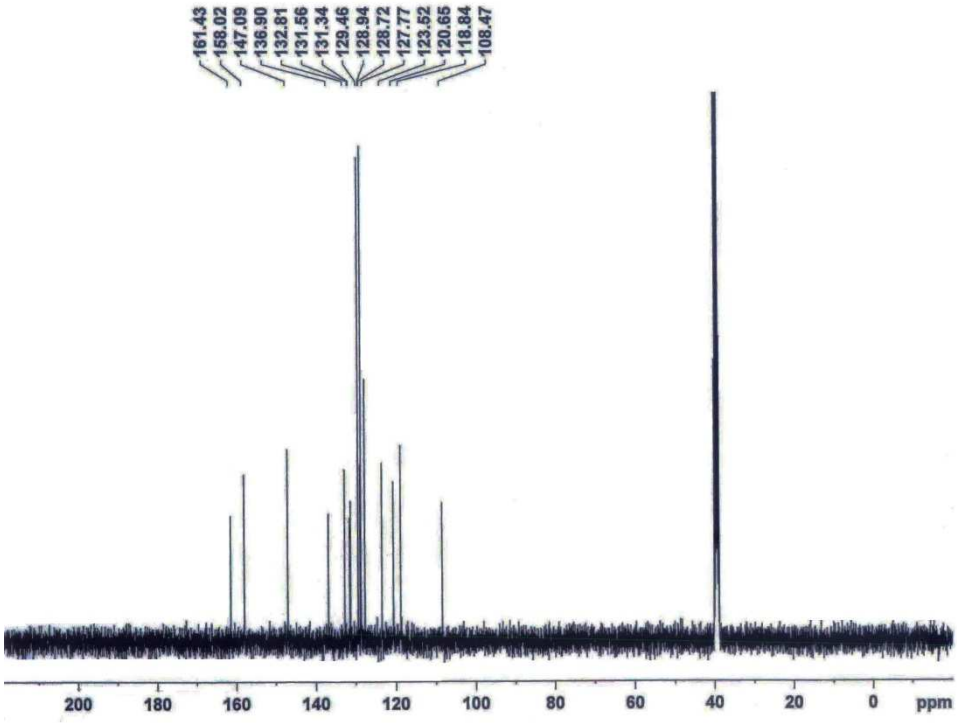

Figure S8: ^{13}C NMR for L_4

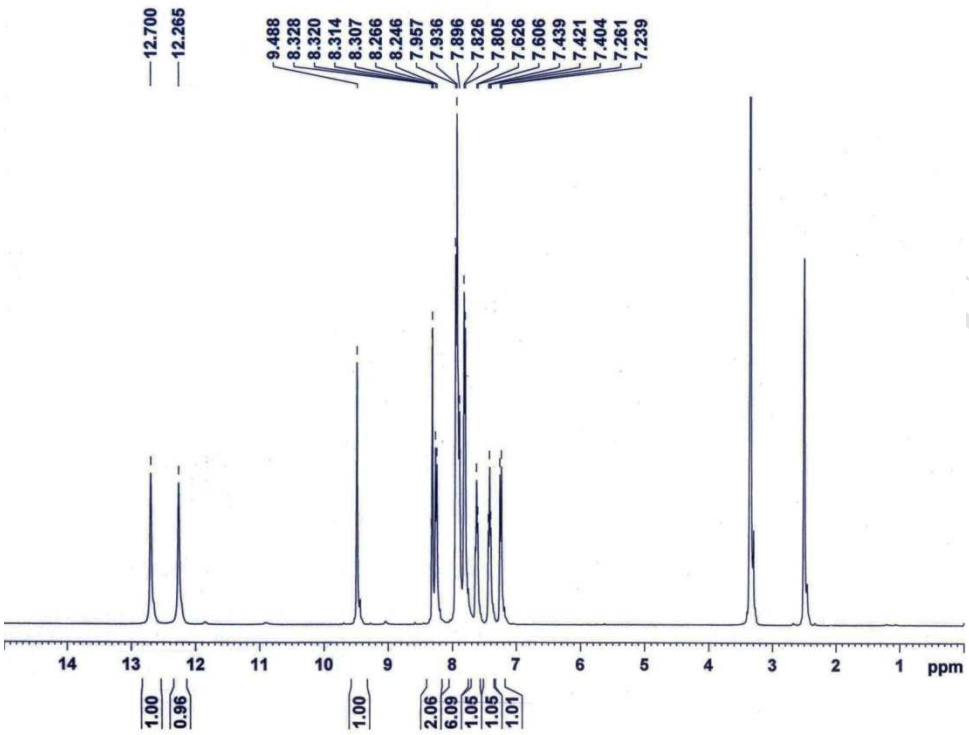

Figure S9: ^{1}H NMR for L_5

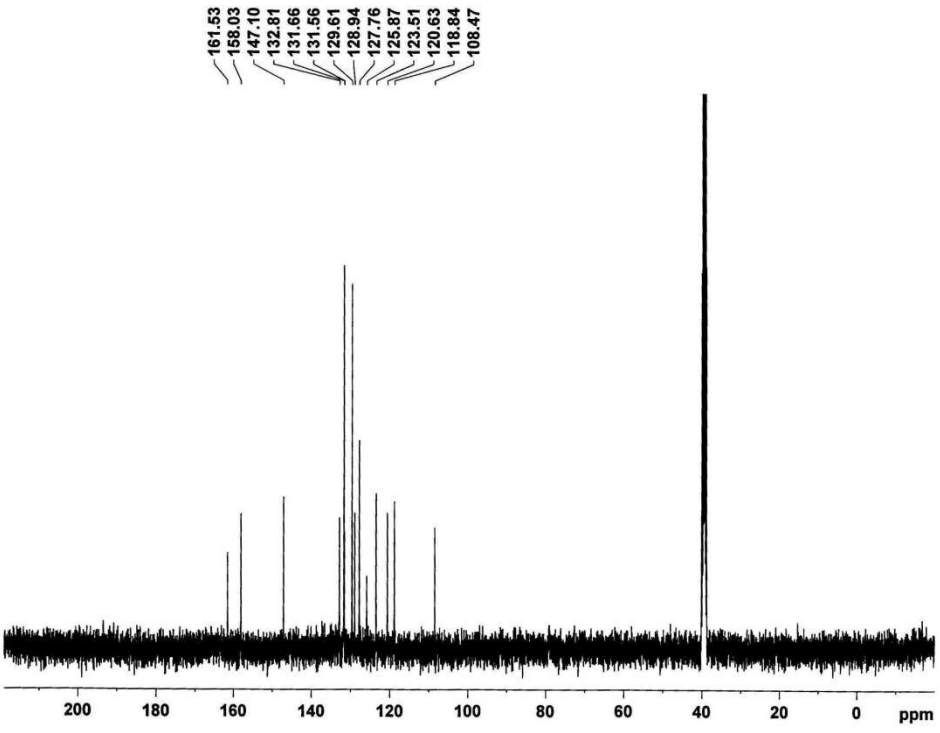

Figure S10: ^{13}C NMR for L_5

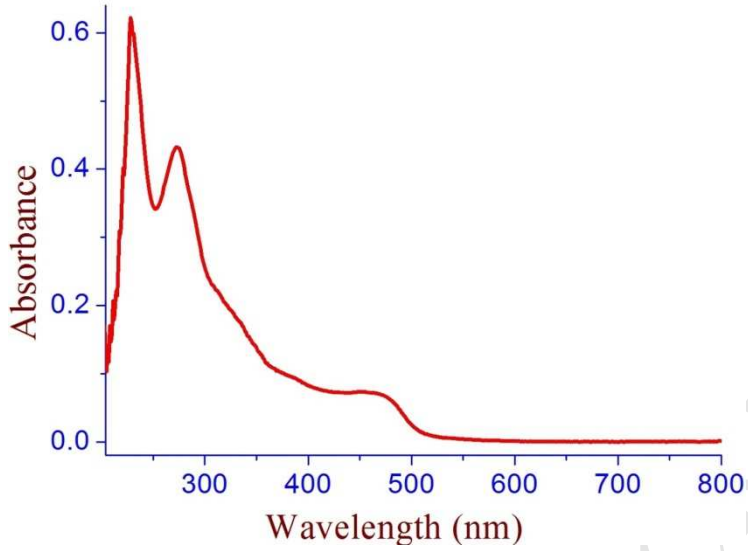

Figure S11. Electronic spectrum of complex **1**

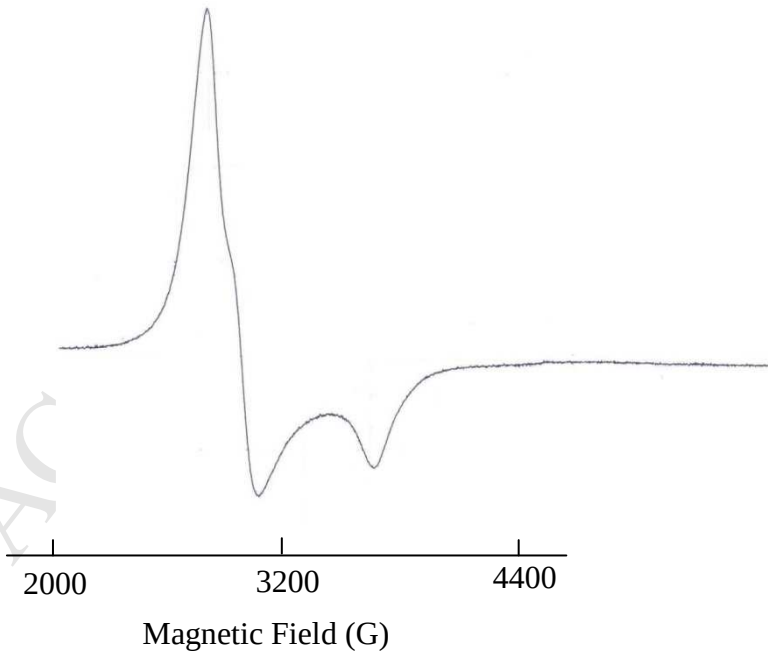

Figure S12. EPR spectrum of complex **2** at LNT

Table 4. Atomic coordinates (x 10^4) and equivalent isotropic displacement parameters ($Å^2$x 10^3) for complex 1. U(eq) is defined as one third of the trace of the orthogonalized U^{ij} tensor.

	x	y	z	U(eq)
Ru(1)	4452(1)	2705(1)	2688(1)	19(1)
Cl(1)	4658(1)	1496(1)	3039(1)	30(1)
P(1)	2778(1)	2739(1)	3090(1)	20(1)
P(2)	6119(1)	2612(1)	2278(1)	23(1)
O(1)	3622(1)	2568(1)	1707(1)	28(1)
O(2)	5387(1)	3081(1)	3602(1)	21(1)
N(1)	4343(1)	3761(1)	2543(1)	20(1)
N(2)	4948(2)	4179(1)	3088(1)	24(1)
C(1)	3772(2)	4105(1)	2012(1)	24(1)
C(2)	3093(2)	3792(1)	1402(1)	24(1)
C(3)	3039(2)	3051(1)	1288(1)	25(1)
C(4)	2349(2)	2774(1)	668(1)	33(1)
C(5)	1774(2)	3212(2)	168(1)	36(1)
C(6)	1813(2)	3962(2)	246(1)	32(1)
C(7)	2451(2)	4260(1)	874(1)	28(1)
C(8)	1219(2)	4421(2)	-278(1)	44(1)
C(9)	1225(2)	5135(2)	-189(1)	51(1)
C(10)	1824(2)	5436(2)	437(1)	47(1)
C(11)	2416(2)	5006(1)	953(1)	36(1)
C(12)	5437(2)	3772(1)	3603(1)	20(1)
C(13)	6116(2)	4125(1)	4229(1)	22(1)
C(14)	5876(2)	4809(1)	4415(1)	28(1)
C(15)	6524(2)	5133(1)	4998(1)	33(1)
C(16)	7421(2)	4780(1)	5390(1)	38(1)
C(17)	7673(2)	4102(1)	5204(1)	48(1)
C(18)	7015(2)	3770(1)	4626(1)	39(1)
C(19)	1895(2)	1957(1)	2873(1)	28(1)
C(20)	1913(2)	1567(1)	2275(2)	41(1)
C(21)	1153(2)	1018(2)	2076(2)	56(1)
C(22)	390(2)	864(1)	2455(2)	55(1)
C(23)	374(2)	1246(1)	3045(2)	48(1)
C(24)	1134(2)	1789(1)	3258(1)	35(1)
C(25)	1817(2)	3457(1)	2741(1)	22(1)

C(26)	848(2)	3323(1)	2246(1)	27(1)
C(27)	155(2)	3881(1)	1963(1)	33(1)
C(28)	422(2)	4573(1)	2168(1)	34(1)
C(29)	1390(2)	4715(1)	2654(1)	31(1)
C(30)	2088(2)	4165(1)	2937(1)	26(1)
C(31)	2986(2)	2810(1)	4036(1)	23(1)
C(32)	2280(2)	3186(1)	4358(1)	28(1)
C(33)	2447(2)	3192(1)	5077(1)	37(1)
C(34)	3323(2)	2819(2)	5480(1)	44(1)
C(35)	4028(2)	2445(2)	5167(1)	41(1)
C(36)	3866(2)	2437(1)	4449(1)	31(1)
C(37)	7376(2)	2692(1)	2964(1)	29(1)
C(38)	7513(2)	2207(1)	3514(1)	34(1)
C(39)	8446(2)	2230(2)	4053(1)	41(1)
C(40)	9236(2)	2749(2)	4058(1)	48(1)
C(41)	9110(2)	3230(2)	3518(2)	49(1)
C(42)	8188(2)	3200(2)	2965(1)	38(1)
C(43)	6206(2)	3287(1)	1625(1)	29(1)
C(44)	6306(2)	4005(1)	1818(1)	36(1)
C(45)	6326(3)	4528(2)	1326(2)	48(1)
C(46)	6220(3)	4348(2)	634(2)	57(1)
C(47)	6101(3)	3644(2)	440(2)	62(1)
C(48)	6094(2)	3115(2)	929(1)	44(1)
C(49)	6308(2)	1755(1)	1875(1)	26(1)
C(50)	7331(2)	1438(2)	1957(1)	36(1)
C(51)	7444(2)	781(2)	1664(1)	47(1)
C(52)	6548(2)	426(2)	1286(1)	43(1)
C(53)	5528(2)	729(2)	1202(2)	50(1)
C(54)	5404(2)	1389(2)	1495(2)	44(1)

Table 5. Atomic coordinates (x 10^4) and equivalent isotropic displacement parameters ($Å^2$x 10^3) For complex 3. U(eq) is defined as one third of the trace of the orthogonalized U^{ij} tensor.

	x	y	z	U(eq)
Ru(1)	4708(1)	4392(1)	4960(1)	16(1)
Cl(1)	5208(1)	3019(1)	5328(1)	26(1)
P(2)	5369(1)	4378(1)	3357(1)	16(1)
P(1)	4024(1)	4451(1)	6556(1)	16(1)
O(1)	2959(3)	4284(2)	3919(3)	22(1)
O(2)	6399(3)	4752(2)	6002(3)	18(1)
O(3)	11129(3)	6841(2)	8525(3)	38(1)
N(1)	4562(3)	5584(2)	4803(3)	19(1)
N(2)	5594(3)	6020(2)	5474(3)	22(1)
C(1)	3633(4)	6001(3)	4159(4)	20(1)
C(2)	2533(4)	5669(3)	3336(4)	21(1)
C(3)	2313(4)	4840(3)	3195(4)	20(1)
C(4)	1329(4)	4545(3)	2221(4)	26(1)
C(5)	576(4)	5060(3)	1435(4)	29(1)
C(6)	700(4)	5904(3)	1577(4)	28(1)
C(7)	1667(4)	6218(3)	2542(4)	23(1)
C(8)	-118(5)	6435(4)	780(5)	37(1)
C(9)	6(5)	7254(4)	914(5)	39(1)
C(10)	936(5)	7559(3)	1872(5)	37(1)
C(11)	1747(5)	7059(3)	2664(5)	29(1)
C(12)	6491(4)	5526(3)	6016(4)	20(1)
C(13)	7700(4)	5887(3)	6689(4)	21(1)
C(14)	7911(4)	6698(3)	6593(4)	24(1)
C(15)	9037(5)	7042(3)	7198(4)	25(1)
C(16)	9974(4)	6570(3)	7905(4)	29(1)
C(17)	9774(5)	5753(3)	8011(5)	35(1)
C(18)	8658(4)	5415(3)	7411(4)	29(1)
C(19)	11370(5)	7675(3)	8433(5)	40(1)
C(38)	7032(3)	4364(4)	3732(3)	23(1)
C(43)	7618(4)	4797(3)	3125(4)	30(1)
C(42)	8863(5)	4694(3)	3356(4)	37(1)
C(41)	9530(4)	4160(3)	4179(5)	37(2)

C(40)	8972(5)	3753(3)	4826(5)	34(1)
C(39)	7730(4)	3858(3)	4609(4)	27(1)
C(44)	4835(5)	5241(3)	2408(4)	21(1)
C(49)	3846(4)	5163(3)	1372(4)	26(1)
C(48)	3354(5)	5846(4)	730(4)	35(1)
C(47)	3833(6)	6595(4)	1105(5)	40(2)
C(46)	4824(5)	6673(3)	2111(5)	37(1)
C(45)	5317(5)	6000(3)	2764(4)	29(1)
C(50)	4861(5)	3531(3)	2369(4)	20(1)
C(55)	3970(5)	3004(3)	2409(4)	31(1)
C(54)	3577(6)	2385(3)	1611(5)	40(1)
C(53)	4059(6)	2307(4)	770(5)	38(1)
C(52)	4944(5)	2838(4)	711(5)	39(1)
C(51)	5359(5)	3442(3)	1516(4)	30(1)
C(26)	3044(5)	5323(3)	6463(4)	20(1)
C(27)	1767(4)	5226(3)	6112(4)	28(1)
C(28)	1003(5)	5888(3)	5864(5)	36(1)
C(29)	1483(5)	6650(3)	5976(5)	36(1)
C(30)	2744(5)	6759(3)	6351(4)	31(1)
C(31)	3517(4)	6098(3)	6589(4)	25(1)
C(20)	3104(4)	3606(3)	6742(4)	20(1)
C(25)	2944(5)	3501(3)	7775(4)	33(1)
C(24)	2222(5)	2879(4)	7907(5)	40(1)
C(23)	1658(5)	2355(3)	7018(5)	35(1)
C(22)	1838(5)	2450(3)	5996(5)	31(1)
C(21)	2556(4)	3079(3)	5858(4)	26(1)
C(32)	5258(4)	4531(3)	7946(4)	23(1)
C(37)	6276(4)	4038(3)	8159(4)	27(1)
C(36)	7224(5)	4060(3)	9220(4)	34(1)
C(35)	7166(4)	4569(3)	10058(4)	35(2)
C(34)	6160(5)	5065(3)	9857(4)	32(1)
C(33)	5204(4)	5054(3)	8803(4)	27(1)

Table 6. Anisotropic displacement parameters ($Å^2 x\ 10^3$) for complex 1. The anisotropic displacement factor exponent takes the form: $-2\pi^2[\ h^2\ a^{*2}U^{11} + ...\ + 2\ h\ k\ a^*\ b^*\ U^{12}\ ]$

	U^{11}	U^{22}	U^{33}	U^{23}	U^{13}	U^{12}
Ru(1)	18(1)	18(1)	18(1)	-4(1)	-1(1)	0(1)
Cl(1)	28(1)	21(1)	38(1)	-3(1)	3(1)	2(1)
P(1)	18(1)	17(1)	22(1)	-4(1)	2(1)	-1(1)
P(2)	20(1)	29(1)	20(1)	-4(1)	2(1)	0(1)
O(1)	30(1)	28(1)	22(1)	-10(1)	-4(1)	3(1)
O(2)	22(1)	19(1)	18(1)	-1(1)	-1(1)	-2(1)
N(1)	22(1)	21(1)	15(1)	-4(1)	0(1)	-2(1)
N(2)	31(1)	21(1)	15(1)	-2(1)	-3(1)	-4(1)
C(1)	27(1)	25(1)	17(1)	-2(1)	1(1)	1(1)
C(2)	23(1)	32(1)	15(1)	-1(1)	2(1)	2(1)
C(3)	21(1)	34(1)	18(1)	-6(1)	1(1)	2(1)
C(4)	29(1)	42(1)	24(1)	-12(1)	-1(1)	-1(1)
C(5)	28(1)	58(2)	18(1)	-12(1)	-2(1)	-3(1)
C(6)	25(1)	53(2)	18(1)	1(1)	2(1)	0(1)
C(7)	24(1)	41(1)	17(1)	1(1)	2(1)	1(1)
C(8)	37(2)	68(2)	21(1)	5(1)	-4(1)	0(1)
C(9)	48(2)	68(2)	29(1)	19(1)	-6(1)	9(2)
C(10)	51(2)	47(2)	37(2)	14(1)	-1(1)	7(1)
C(11)	40(2)	42(2)	22(1)	7(1)	-2(1)	4(1)
C(12)	22(1)	21(1)	17(1)	-1(1)	3(1)	-3(1)
C(13)	27(1)	21(1)	15(1)	0(1)	1(1)	-8(1)
C(14)	27(1)	28(1)	26(1)	-5(1)	3(1)	-4(1)
C(15)	36(1)	31(1)	33(1)	-12(1)	9(1)	-9(1)
C(16)	49(2)	34(1)	24(1)	-7(1)	-5(1)	-16(1)
C(17)	58(2)	33(1)	37(2)	2(1)	-25(1)	-4(1)
C(18)	51(2)	22(1)	31(1)	-1(1)	-15(1)	-2(1)
C(19)	19(1)	17(1)	42(1)	-3(1)	-3(1)	1(1)
C(20)	28(1)	34(1)	57(2)	-21(1)	1(1)	-2(1)
C(21)	31(2)	39(2)	88(2)	-35(2)	-7(2)	2(1)
C(22)	22(1)	22(1)	110(3)	-15(2)	-8(2)	-1(1)
C(23)	25(1)	28(1)	87(2)	7(2)	5(1)	-5(1)
C(24)	27(1)	24(1)	51(2)	2(1)	0(1)	-4(1)
C(25)	22(1)	23(1)	21(1)	0(1)	5(1)	2(1)

C(26)	29(1)	26(1)	23(1)	1(1)	1(1)	-1(1)
C(27)	29(1)	38(1)	28(1)	7(1)	-5(1)	2(1)
C(28)	36(1)	31(1)	34(1)	10(1)	3(1)	8(1)
C(29)	39(1)	21(1)	32(1)	-1(1)	7(1)	3(1)
C(30)	27(1)	22(1)	26(1)	-3(1)	4(1)	2(1)
C(31)	24(1)	21(1)	25(1)	0(1)	5(1)	-5(1)
C(32)	26(1)	26(1)	31(1)	1(1)	8(1)	-2(1)
C(33)	41(2)	41(1)	33(1)	-1(1)	16(1)	1(1)
C(34)	48(2)	61(2)	25(1)	5(1)	14(1)	1(1)
C(35)	39(2)	57(2)	28(1)	12(1)	8(1)	9(1)
C(36)	28(1)	36(1)	29(1)	5(1)	7(1)	4(1)
C(37)	21(1)	39(1)	26(1)	-7(1)	3(1)	2(1)
C(38)	24(1)	47(2)	30(1)	-2(1)	5(1)	1(1)
C(39)	28(1)	67(2)	27(1)	2(1)	4(1)	7(1)
C(40)	21(1)	85(2)	34(1)	-10(2)	-2(1)	2(1)
C(41)	28(1)	70(2)	47(2)	-7(2)	0(1)	-13(1)
C(42)	26(1)	50(2)	37(1)	-1(1)	3(1)	-7(1)
C(43)	25(1)	38(1)	24(1)	-1(1)	6(1)	1(1)
C(44)	42(2)	38(1)	31(1)	0(1)	14(1)	-2(1)
C(45)	55(2)	39(2)	57(2)	6(1)	27(2)	1(1)
C(46)	74(2)	57(2)	46(2)	20(2)	25(2)	9(2)
C(47)	94(3)	63(2)	32(2)	5(2)	21(2)	4(2)
C(48)	54(2)	49(2)	29(1)	-2(1)	12(1)	2(1)
C(49)	26(1)	31(1)	23(1)	-2(1)	7(1)	3(1)
C(50)	29(1)	52(2)	26(1)	-9(1)	3(1)	7(1)
C(51)	43(2)	61(2)	35(1)	-10(1)	1(1)	26(1)
C(52)	53(2)	39(2)	40(2)	-8(1)	16(1)	12(1)
C(53)	40(2)	48(2)	62(2)	-30(2)	12(1)	-6(1)
C(54)	26(1)	49(2)	56(2)	-22(1)	6(1)	3(1)

Table 7. Anisotropic displacement parameters ($Å^2 x\ 10^3$) for complex 3. The anisotropic displacement factor exponent takes the form: $-2\pi^2[\ h^2\ a^{*2}U^{11} + ...\ + 2\ h\ k\ a^*\ b^*\ U^{12}\ ]$

	U^{11}	U^{22}	U^{33}	U^{23}	U^{13}	U^{12}
Ru(1)	20(1)	13(1)	13(1)	0(1)	4(1)	0(1)
Cl(1)	33(1)	17(1)	26(1)	1(1)	9(1)	2(1)
P(2)	17(1)	18(1)	12(1)	-1(1)	4(1)	-1(1)
P(1)	18(1)	16(1)	12(1)	0(1)	4(1)	-1(1)
O(1)	23(1)	20(2)	22(2)	1(2)	5(1)	-2(2)
O(2)	24(2)	15(2)	14(2)	-1(1)	3(1)	-1(1)
O(3)	30(2)	43(2)	30(2)	2(2)	-4(2)	-12(2)
N(1)	23(2)	21(2)	13(2)	-3(2)	7(2)	-5(2)
N(2)	22(2)	21(2)	19(2)	3(2)	2(2)	6(2)
C(1)	21(2)	19(2)	18(2)	3(2)	6(2)	1(2)
C(2)	20(2)	25(2)	17(2)	0(2)	7(2)	2(2)
C(3)	19(2)	27(3)	15(2)	3(2)	6(2)	0(2)
C(4)	21(2)	35(4)	20(2)	-2(2)	4(2)	-6(2)
C(5)	19(2)	44(3)	19(2)	-3(2)	2(2)	-4(2)
C(6)	19(2)	41(3)	23(3)	10(2)	8(2)	6(2)
C(7)	20(2)	29(2)	22(3)	6(2)	9(2)	5(2)
C(8)	27(3)	59(4)	24(3)	14(3)	7(2)	7(2)
C(9)	33(3)	50(4)	35(3)	23(3)	11(3)	19(3)
C(10)	34(3)	37(3)	42(4)	15(3)	17(3)	13(2)
C(11)	25(3)	32(3)	28(3)	9(2)	7(2)	7(2)
C(12)	25(2)	21(2)	15(2)	1(2)	9(2)	-3(2)
C(13)	20(2)	25(2)	15(2)	-2(2)	4(2)	-2(2)
C(14)	22(2)	23(3)	25(3)	0(2)	5(2)	2(2)
C(15)	32(3)	17(3)	23(3)	-4(2)	6(2)	-8(2)
C(16)	24(2)	39(3)	19(3)	-3(2)	2(2)	-4(2)
C(17)	26(3)	35(3)	32(3)	10(2)	-4(2)	2(2)
C(18)	30(3)	22(3)	30(3)	2(2)	2(2)	-5(2)
C(19)	32(3)	37(3)	42(4)	-7(3)	1(3)	-16(2)
C(38)	22(2)	27(2)	17(2)	-9(3)	4(2)	-4(3)
C(43)	27(3)	44(3)	19(3)	-2(2)	7(2)	-2(2)
C(42)	29(3)	55(4)	26(3)	-12(2)	11(2)	-8(2)
C(41)	18(2)	53(4)	35(3)	-18(2)	5(2)	-2(2)
C(40)	26(3)	35(3)	31(3)	-10(2)	-1(2)	6(2)

C(39)	25(3)	28(3)	24(3)	-3(2)	5(2)	2(2)
C(44)	26(3)	20(3)	17(3)	2(2)	10(2)	2(2)
C(49)	25(2)	33(3)	22(3)	4(2)	9(2)	2(2)
C(48)	29(3)	49(4)	26(3)	16(3)	8(2)	5(2)
C(47)	46(3)	36(3)	43(4)	25(3)	21(3)	12(3)
C(46)	50(3)	29(3)	41(3)	10(2)	26(3)	0(3)
C(45)	38(3)	27(3)	26(3)	2(2)	15(2)	-5(2)
C(50)	24(3)	20(3)	12(3)	-3(2)	1(2)	2(2)
C(55)	45(3)	29(3)	21(3)	-7(2)	14(2)	-8(2)
C(54)	57(4)	32(3)	26(3)	-4(2)	9(3)	-15(3)
C(53)	54(4)	28(3)	27(3)	-10(2)	7(3)	0(3)
C(52)	46(3)	43(3)	28(3)	-11(2)	14(3)	5(3)
C(51)	32(3)	32(3)	28(3)	-4(2)	11(2)	-3(2)
C(26)	26(3)	22(3)	14(2)	-2(2)	9(2)	1(2)
C(27)	29(3)	24(3)	27(3)	-5(2)	6(2)	2(2)
C(28)	25(3)	36(3)	43(3)	-6(3)	5(2)	2(2)
C(29)	38(3)	29(3)	39(3)	-1(2)	13(3)	10(3)
C(30)	45(3)	16(3)	30(3)	-2(2)	11(3)	3(2)
C(31)	28(2)	23(3)	22(3)	0(2)	9(2)	2(2)
C(20)	21(3)	19(3)	21(3)	5(2)	8(2)	3(2)
C(25)	39(3)	35(3)	25(3)	-3(2)	11(2)	-11(2)
C(24)	42(3)	53(4)	30(3)	12(3)	18(3)	-10(3)
C(23)	34(3)	33(3)	37(3)	8(2)	11(3)	-8(2)
C(22)	31(3)	25(3)	36(3)	0(2)	11(2)	-4(2)
C(21)	27(2)	24(3)	28(3)	-2(2)	9(2)	-3(2)
C(32)	25(2)	26(3)	15(2)	3(2)	5(2)	-2(2)
C(37)	28(3)	32(3)	18(2)	5(2)	7(2)	4(2)
C(36)	24(3)	55(3)	21(3)	9(2)	6(2)	8(2)
C(35)	27(2)	56(5)	16(2)	6(2)	1(2)	-4(2)
C(34)	40(3)	35(3)	17(2)	-4(2)	7(2)	-4(2)
C(33)	32(3)	28(3)	17(2)	3(2)	5(2)	7(2)

Table 8. Hydrogen coordinates (x 10^4) and isotropic displacement parameters ($Å^2$x 10^3) for complex 1.

	x	y	z	U(eq)
H(1)	3807	4611	2029	28
H(4)	2290	2272	602	39
H(5)	1335	3011	-244	43
H(8)	808	4222	-701	53
H(9)	826	5434	-549	61
H(10)	1820	5938	504	56
H(11)	2811	5217	1373	44
H(14)	5265	5057	4141	33
H(15)	6348	5599	5126	40
H(16)	7866	5003	5789	46
H(17)	8297	3861	5472	58
H(18)	7183	3300	4503	46
H(20)	2435	1673	2007	50
H(21)	1165	746	1671	67
H(22)	-128	492	2309	66
H(23)	-156	1140	3308	58
H(24)	1131	2047	3672	43
H(26)	658	2848	2102	32
H(27)	-504	3785	1626	40
H(28)	-57	4952	1977	41
H(29)	1575	5193	2793	37
H(30)	2754	4268	3265	31
H(32)	1679	3442	4083	33
H(33)	1962	3451	5293	44
H(34)	3437	2822	5973	52
H(35)	4629	2191	5446	49
H(36)	4355	2177	4237	37
H(38)	6964	1858	3519	41
H(39)	8543	1890	4419	49
H(40)	9865	2774	4433	58
H(41)	9656	3584	3522	59
H(42)	8114	3527	2589	46

H(44)	6362	4135	2290	43
H(45)	6414	5014	1464	58
H(46)	6229	4707	295	69
H(47)	6022	3518	-36	74
H(48)	6013	2630	786	52
H(50)	7964	1675	2217	43
H(51)	8154	574	1726	57
H(52)	6632	-24	1085	52
H(53)	4901	486	941	60
H(54)	4691	1592	1434	53

Table 9. Hydrogen coordinates (x 10^4) and isotropic displacement parameters ($Å^2$x 10^3) for complex 3.

	x	y	z	U(eq)
H(1)	3684	6570	4236	24
H(4)	1199	3981	2120	31
H(5)	-47	4847	777	35
H(8)	-765	6221	141	45
H(9)	-532	7607	364	47
H(10)	1013	8126	1982	44
H(11)	2373	7287	3307	35
H(14)	7270	7026	6102	29
H(15)	9165	7601	7127	30
H(17)	10417	5428	8504	42
H(18)	8534	4856	7486	35
H(19A)	11204	7810	7630	61
H(19B)	12233	7789	8886	61
H(19C)	10840	7998	8719	61
H(43)	7162	5166	2550	36
H(42)	9256	4995	2941	44
H(41)	10373	4070	4305	44
H(40)	9441	3401	5420	41
H(39)	7354	3584	5061	32
H(49)	3512	4647	1110	32
H(48)	2683	5794	26	42
H(47)	3478	7060	670	48
H(46)	5169	7189	2357	45
H(45)	5993	6058	3463	35
H(55)	3621	3062	2982	37
H(54)	2972	2015	1651	48
H(53)	3783	1886	225	46
H(52)	5267	2788	118	46
H(51)	5985	3798	1489	36
H(27)	1426	4700	6045	33
H(28)	138	5816	5613	44
H(29)	952	7104	5796	43

H(30)	3077	7288	6445	37
H(31)	4380	6175	6841	29
H(25)	3331	3858	8393	39
H(24)	2112	2811	8616	48
H(23)	1151	1934	7108	42
H(22)	1470	2084	5386	37
H(21)	2671	3146	5150	32
H(37)	6325	3685	7581	32
H(36)	7917	3720	9364	41
H(35)	7819	4581	10779	42
H(34)	6122	5416	10442	38
H(33)	4517	5400	8664	32

Table 10. Torsion angles [°] for complex 1.

Ru(1)-P(1)-C(19)-C(20)	-28.8(2)
Ru(1)-P(1)-C(19)-C(24)	157.48(16)
Ru(1)-P(1)-C(25)-C(26)	106.54(18)
Ru(1)-P(1)-C(25)-C(30)	-69.25(19)
Ru(1)-P(1)-C(31)-C(32)	145.72(17)
Ru(1)-P(1)-C(31)-C(36)	-37.5(2)
Ru(1)-P(2)-C(37)-C(38)	57.6(2)
Ru(1)-P(2)-C(37)-C(42)	-122.7(2)
Ru(1)-P(2)-C(43)-C(44)	66.7(2)
Ru(1)-P(2)-C(43)-C(48)	-108.5(2)
Ru(1)-P(2)-C(49)-C(50)	-143.29(18)
Ru(1)-P(2)-C(49)-C(54)	34.3(2)
Ru(1)-O(1)-C(3)-C(2)	15.1(3)
Ru(1)-O(1)-C(3)-C(4)	-167.54(16)
Ru(1)-O(2)-C(12)-N(2)	0.3(3)
Ru(1)-O(2)-C(12)-C(13)	-178.39(15)
Ru(1)-N(1)-N(2)-C(12)	-2.6(2)
Ru(1)-N(1)-C(1)-C(2)	-0.6(3)
P(1)-C(19)-C(20)-C(21)	-173.2(2)
P(1)-C(19)-C(24)-C(23)	172.29(19)
P(1)-C(25)-C(26)-C(27)	-176.89(18)

P(1)-C(25)-C(30)-C(29)	177.30(18)
P(1)-C(31)-C(32)-C(33)	176.70(18)
P(1)-C(31)-C(36)-C(35)	-176.9(2)
P(2)-C(37)-C(38)-C(39)	179.7(2)
P(2)-C(37)-C(42)-C(41)	178.8(2)
P(2)-C(43)-C(44)-C(45)	-177.2(2)
P(2)-C(43)-C(48)-C(47)	176.3(2)
P(2)-C(49)-C(50)-C(51)	178.1(2)
P(2)-C(49)-C(54)-C(53)	-178.2(2)
O(1)-C(3)-C(4)-C(5)	-174.8(2)
O(2)-C(12)-C(13)-C(14)	-152.4(2)
O(2)-C(12)-C(13)-C(18)	28.8(3)
N(1)-N(2)-C(12)-O(2)	1.5(3)
N(1)-N(2)-C(12)-C(13)	-179.83(18)
N(1)-C(1)-C(2)-C(3)	-5.2(4)
N(1)-C(1)-C(2)-C(7)	176.0(2)
N(2)-N(1)-C(1)-C(2)	-179.7(2)
N(2)-C(12)-C(13)-C(14)	28.8(3)
N(2)-C(12)-C(13)-C(18)	-150.0(2)
C(1)-N(1)-N(2)-C(12)	176.65(19)
C(1)-C(2)-C(3)-O(1)	-2.5(4)
C(1)-C(2)-C(3)-C(4)	-179.7(2)
C(1)-C(2)-C(7)-C(6)	176.8(2)
C(1)-C(2)-C(7)-C(11)	-3.8(3)
C(2)-C(3)-C(4)-C(5)	2.7(4)
C(2)-C(7)-C(11)-C(10)	178.3(2)
C(3)-C(2)-C(7)-C(6)	-2.1(3)
C(3)-C(2)-C(7)-C(11)	177.3(2)
C(3)-C(4)-C(5)-C(6)	-1.4(4)
C(4)-C(5)-C(6)-C(7)	-1.7(4)
C(4)-C(5)-C(6)-C(8)	179.5(2)
C(5)-C(6)-C(7)-C(2)	3.4(3)
C(5)-C(6)-C(7)-C(11)	-176.1(2)
C(5)-C(6)-C(8)-C(9)	177.4(3)
C(6)-C(7)-C(11)-C(10)	-2.3(4)
C(6)-C(8)-C(9)-C(10)	-0.5(5)
C(7)-C(2)-C(3)-O(1)	176.3(2)
C(7)-C(2)-C(3)-C(4)	-0.9(3)

C(7)-C(6)-C(8)-C(9)	-1.5(4)
C(8)-C(6)-C(7)-C(2)	-177.8(2)
C(8)-C(6)-C(7)-C(11)	2.8(3)
C(8)-C(9)-C(10)-C(11)	1.0(5)
C(9)-C(10)-C(11)-C(7)	0.4(4)
C(12)-C(13)-C(14)-C(15)	-179.5(2)
C(12)-C(13)-C(18)-C(17)	178.5(2)
C(13)-C(14)-C(15)-C(16)	1.0(4)
C(14)-C(13)-C(18)-C(17)	-0.3(4)
C(14)-C(15)-C(16)-C(17)	-0.2(4)
C(15)-C(16)-C(17)-C(18)	-0.8(4)
C(16)-C(17)-C(18)-C(13)	1.1(4)
C(18)-C(13)-C(14)-C(15)	-0.7(3)
C(19)-P(1)-C(25)-C(26)	-18.9(2)
C(19)-P(1)-C(25)-C(30)	165.27(18)
C(19)-P(1)-C(31)-C(32)	-88.3(2)
C(19)-P(1)-C(31)-C(36)	88.48(19)
C(19)-C(20)-C(21)-C(22)	0.6(4)
C(20)-C(19)-C(24)-C(23)	-1.4(4)
C(20)-C(21)-C(22)-C(23)	-0.8(5)
C(21)-C(22)-C(23)-C(24)	-0.1(4)
C(22)-C(23)-C(24)-C(19)	1.2(4)
C(24)-C(19)-C(20)-C(21)	0.5(4)
C(25)-P(1)-C(19)-C(20)	97.2(2)
C(25)-P(1)-C(19)-C(24)	-76.4(2)
C(25)-P(1)-C(31)-C(32)	17.5(2)
C(25)-P(1)-C(31)-C(36)	-165.74(18)
C(25)-C(26)-C(27)-C(28)	0.0(4)
C(26)-C(25)-C(30)-C(29)	1.4(3)
C(26)-C(27)-C(28)-C(29)	0.7(4)
C(27)-C(28)-C(29)-C(30)	-0.4(4)
C(28)-C(29)-C(30)-C(25)	-0.7(4)
C(30)-C(25)-C(26)-C(27)	-1.0(3)
C(31)-P(1)-C(19)-C(20)	-154.1(2)
C(31)-P(1)-C(19)-C(24)	32.2(2)
C(31)-P(1)-C(25)-C(26)	-126.50(19)
C(31)-P(1)-C(25)-C(30)	57.7(2)
C(31)-C(32)-C(33)-C(34)	-0.1(4)

C(32)-C(31)-C(36)-C(35)	0.0(4)
C(32)-C(33)-C(34)-C(35)	0.2(4)
C(33)-C(34)-C(35)-C(36)	-0.2(4)
C(34)-C(35)-C(36)-C(31)	0.1(4)
C(36)-C(31)-C(32)-C(33)	0.0(3)
C(37)-P(2)-C(43)-C(44)	-59.0(2)
C(37)-P(2)-C(43)-C(48)	125.8(2)
C(37)-P(2)-C(49)-C(50)	-19.1(2)
C(37)-P(2)-C(49)-C(54)	158.5(2)
C(37)-C(38)-C(39)-C(40)	1.7(4)
C(38)-C(37)-C(42)-C(41)	-1.5(4)
C(38)-C(39)-C(40)-C(41)	-1.8(4)
C(39)-C(40)-C(41)-C(42)	0.3(5)
C(40)-C(41)-C(42)-C(37)	1.4(4)
C(42)-C(37)-C(38)-C(39)	0.0(4)
C(43)-P(2)-C(37)-C(38)	-177.71(18)
C(43)-P(2)-C(37)-C(42)	2.0(2)
C(43)-P(2)-C(49)-C(50)	92.4(2)
C(43)-P(2)-C(49)-C(54)	-90.0(2)
C(43)-C(44)-C(45)-C(46)	1.6(4)
C(44)-C(43)-C(48)-C(47)	1.0(4)
C(44)-C(45)-C(46)-C(47)	-0.4(5)
C(45)-C(46)-C(47)-C(48)	-0.5(5)
C(46)-C(47)-C(48)-C(43)	0.1(5)
C(48)-C(43)-C(44)-C(45)	-1.9(4)
C(49)-P(2)-C(37)-C(38)	-66.9(2)
C(49)-P(2)-C(37)-C(42)	112.8(2)
C(49)-P(2)-C(43)-C(44)	-167.7(2)
C(49)-P(2)-C(43)-C(48)	17.1(2)
C(49)-C(50)-C(51)-C(52)	-0.1(4)
C(50)-C(49)-C(54)-C(53)	-0.5(4)
C(50)-C(51)-C(52)-C(53)	-0.2(5)
C(51)-C(52)-C(53)-C(54)	0.1(5)
C(52)-C(53)-C(54)-C(49)	0.3(5)
C(54)-C(49)-C(50)-C(51)	0.4(4)

Symmetry transformations used to generate equivalent atoms:

Table 11. Torsion angles [°] for complex 3.

Ru(1)-P(2)-C(38)-C(43)	-141.3(4)
Ru(1)-P(2)-C(38)-C(39)	43.1(5)
Ru(1)-P(2)-C(44)-C(49)	-102.2(4)
Ru(1)-P(2)-C(44)-C(45)	70.5(4)
Ru(1)-P(2)-C(50)-C(55)	11.5(5)
Ru(1)-P(2)-C(50)-C(51)	-171.4(3)
Ru(1)-P(1)-C(26)-C(27)	103.1(4)
Ru(1)-P(1)-C(26)-C(31)	-68.4(4)
Ru(1)-P(1)-C(20)-C(25)	163.9(4)
Ru(1)-P(1)-C(20)-C(21)	-16.9(5)
Ru(1)-P(1)-C(32)-C(37)	-44.4(4)
Ru(1)-P(1)-C(32)-C(33)	136.9(4)
Ru(1)-O(1)-C(3)-C(2)	-26.9(6)
Ru(1)-O(1)-C(3)-C(4)	153.5(3)
Ru(1)-O(2)-C(12)-N(2)	3.1(5)
Ru(1)-O(2)-C(12)-C(13)	-176.6(3)
Ru(1)-N(1)-N(2)-C(12)	4.6(4)
Ru(1)-N(1)-C(1)-C(2)	-5.8(7)
P(2)-C(38)-C(43)-C(42)	-172.3(4)
P(2)-C(38)-C(39)-C(40)	171.9(4)
P(2)-C(44)-C(49)-C(48)	171.9(4)
P(2)-C(44)-C(45)-C(46)	-172.4(4)
P(2)-C(50)-C(55)-C(54)	177.5(4)
P(2)-C(50)-C(51)-C(52)	-176.1(4)
P(1)-C(26)-C(27)-C(28)	-169.7(4)
P(1)-C(26)-C(31)-C(30)	170.4(4)
P(1)-C(20)-C(25)-C(24)	178.1(4)
P(1)-C(20)-C(21)-C(22)	-178.6(4)
P(1)-C(32)-C(37)-C(36)	-178.0(4)
P(1)-C(32)-C(33)-C(34)	177.8(4)
O(1)-C(3)-C(4)-C(5)	177.9(4)
O(2)-C(12)-C(13)-C(14)	169.7(4)
O(2)-C(12)-C(13)-C(18)	-8.8(6)
O(3)-C(16)-C(17)-C(18)	-178.7(5)
N(1)-N(2)-C(12)-O(2)	-5.2(6)

N(1)-N(2)-C(12)-C(13)	174.5(4)
N(1)-C(1)-C(2)-C(3)	4.4(7)
N(1)-C(1)-C(2)-C(7)	-169.5(4)
N(2)-N(1)-C(1)-C(2)	174.3(4)
N(2)-C(12)-C(13)-C(14)	-10.0(7)
N(2)-C(12)-C(13)-C(18)	171.5(4)
C(1)-N(1)-N(2)-C(12)	-175.4(4)
C(1)-C(2)-C(3)-O(1)	13.0(7)
C(1)-C(2)-C(3)-C(4)	-167.4(4)
C(1)-C(2)-C(7)-C(6)	167.4(4)
C(1)-C(2)-C(7)-C(11)	-11.3(7)
C(2)-C(3)-C(4)-C(5)	-1.7(7)
C(2)-C(7)-C(11)-C(10)	177.6(5)
C(3)-C(2)-C(7)-C(6)	-6.7(6)
C(3)-C(2)-C(7)-C(11)	174.5(4)
C(3)-C(4)-C(5)-C(6)	-2.9(7)
C(4)-C(5)-C(6)-C(7)	2.5(7)
C(4)-C(5)-C(6)-C(8)	-177.4(5)
C(5)-C(6)-C(7)-C(2)	2.3(7)
C(5)-C(6)-C(7)-C(11)	-178.9(4)
C(5)-C(6)-C(8)-C(9)	-179.6(5)
C(6)-C(7)-C(11)-C(10)	-1.1(7)
C(6)-C(8)-C(9)-C(10)	-1.9(8)
C(7)-C(2)-C(3)-O(1)	-173.1(4)
C(7)-C(2)-C(3)-C(4)	6.4(6)
C(7)-C(6)-C(8)-C(9)	0.4(7)
C(8)-C(6)-C(7)-C(2)	-177.8(4)
C(8)-C(6)-C(7)-C(11)	1.1(7)
C(8)-C(9)-C(10)-C(11)	1.8(8)
C(9)-C(10)-C(11)-C(7)	-0.3(8)
C(12)-C(13)-C(14)-C(15)	-178.9(4)
C(12)-C(13)-C(18)-C(17)	178.9(5)
C(13)-C(14)-C(15)-C(16)	0.5(7)
C(14)-C(13)-C(18)-C(17)	0.4(8)
C(14)-C(15)-C(16)-O(3)	178.7(5)
C(14)-C(15)-C(16)-C(17)	-0.6(8)
C(15)-C(16)-C(17)-C(18)	0.6(8)
C(16)-C(17)-C(18)-C(13)	-0.5(8)

C(18)-C(13)-C(14)-C(15)	-0.4(7)
C(19)-O(3)-C(16)-C(15)	0.4(8)
C(19)-O(3)-C(16)-C(17)	179.6(5)
C(38)-P(2)-C(44)-C(49)	131.6(4)
C(38)-P(2)-C(44)-C(45)	-55.6(4)
C(38)-P(2)-C(50)-C(55)	137.9(4)
C(38)-P(2)-C(50)-C(51)	-45.0(5)
C(38)-C(43)-C(42)-C(41)	0.4(8)
C(43)-C(38)-C(39)-C(40)	-3.8(8)
C(43)-C(42)-C(41)-C(40)	-3.4(8)
C(42)-C(41)-C(40)-C(39)	2.8(8)
C(41)-C(40)-C(39)-C(38)	0.9(8)
C(39)-C(38)-C(43)-C(42)	3.2(8)
C(44)-P(2)-C(38)-C(43)	-15.7(5)
C(44)-P(2)-C(38)-C(39)	168.7(4)
C(44)-P(2)-C(50)-C(55)	-113.3(5)
C(44)-P(2)-C(50)-C(51)	63.8(4)
C(44)-C(49)-C(48)-C(47)	-0.1(8)
C(49)-C(44)-C(45)-C(46)	0.5(7)
C(49)-C(48)-C(47)-C(46)	1.5(8)
C(48)-C(47)-C(46)-C(45)	-2.0(8)
C(47)-C(46)-C(45)-C(44)	1.0(8)
C(45)-C(44)-C(49)-C(48)	-0.9(7)
C(50)-P(2)-C(38)-C(43)	90.9(5)
C(50)-P(2)-C(38)-C(39)	-84.7(4)
C(50)-P(2)-C(44)-C(49)	24.6(4)
C(50)-P(2)-C(44)-C(45)	-162.6(5)
C(50)-C(55)-C(54)-C(53)	-1.2(9)
C(55)-C(50)-C(51)-C(52)	1.1(8)
C(55)-C(54)-C(53)-C(52)	0.5(9)
C(54)-C(53)-C(52)-C(51)	1.1(9)
C(53)-C(52)-C(51)-C(50)	-1.8(8)
C(51)-C(50)-C(55)-C(54)	0.5(8)
C(26)-P(1)-C(20)-C(25)	-72.8(4)
C(26)-P(1)-C(20)-C(21)	106.4(4)
C(26)-P(1)-C(32)-C(37)	-167.3(4)
C(26)-P(1)-C(32)-C(33)	14.0(5)
C(26)-C(27)-C(28)-C(29)	-1.1(8)

C(27)-C(26)-C(31)-C(30)	-1.3(7)
C(27)-C(28)-C(29)-C(30)	-0.6(8)
C(28)-C(29)-C(30)-C(31)	1.4(8)
C(29)-C(30)-C(31)-C(26)	-0.4(7)
C(31)-C(26)-C(27)-C(28)	2.1(7)
C(20)-P(1)-C(26)-C(27)	-23.9(5)
C(20)-P(1)-C(26)-C(31)	164.6(4)
C(20)-P(1)-C(32)-C(37)	84.3(4)
C(20)-P(1)-C(32)-C(33)	-94.4(4)
C(20)-C(25)-C(24)-C(23)	0.3(8)
C(25)-C(20)-C(21)-C(22)	0.6(7)
C(25)-C(24)-C(23)-C(22)	1.1(9)
C(24)-C(23)-C(22)-C(21)	-1.5(8)
C(23)-C(22)-C(21)-C(20)	0.7(8)
C(21)-C(20)-C(25)-C(24)	-1.1(8)
C(32)-P(1)-C(26)-C(27)	-132.2(4)
C(32)-P(1)-C(26)-C(31)	56.3(4)
C(32)-P(1)-C(20)-C(25)	36.9(5)
C(32)-P(1)-C(20)-C(21)	-143.9(4)
C(32)-C(37)-C(36)-C(35)	-0.3(8)
C(37)-C(32)-C(33)-C(34)	-0.8(7)
C(37)-C(36)-C(35)-C(34)	0.1(8)
C(36)-C(35)-C(34)-C(33)	-0.3(8)
C(35)-C(34)-C(33)-C(32)	0.6(8)
C(33)-C(32)-C(37)-C(36)	0.7(7)

Symmetry transformations used to generate equivalent atoms:

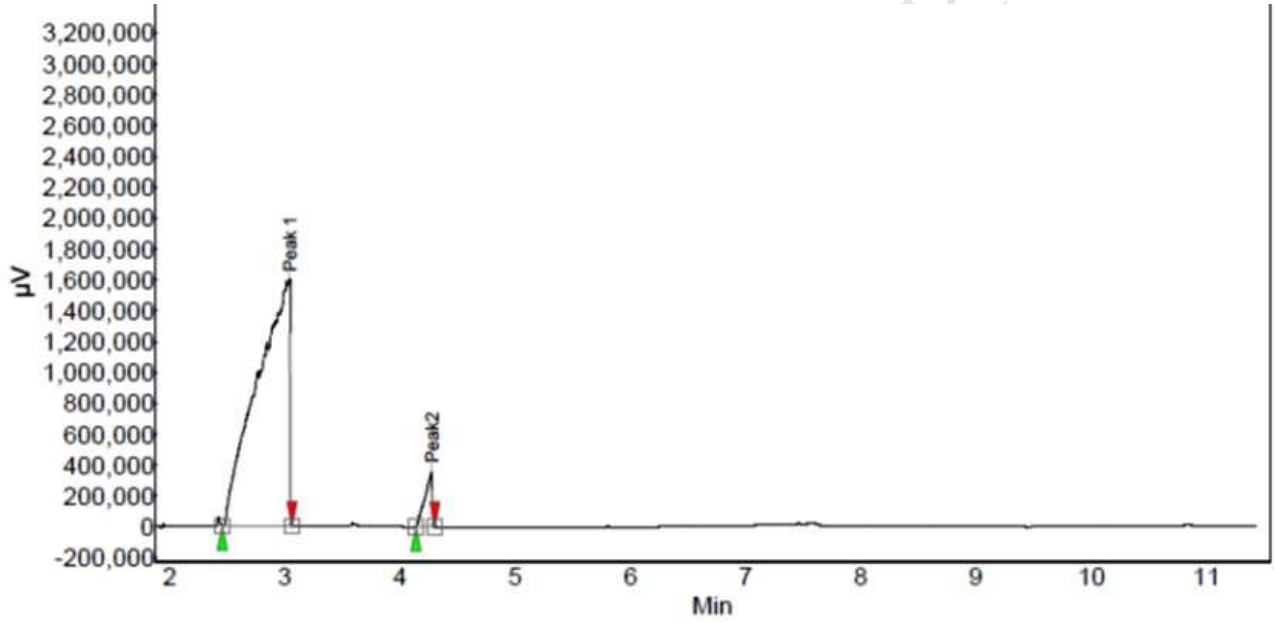

Peak results :

Index	Name	Time [Min]	Quantity [% Area]	Height [µV]	Area [µV.Min]	Area % [%]
1	Peak 1	3.04	95.34	1606595.9	514608.3	95.339
2	Peak2	4.28	4.66	359549.6	25160.8	4.661
Total			100.00	1966145.5	539769.1	100.000

Figure S13. GC Chromatogram for entry **1** in **Table 6**

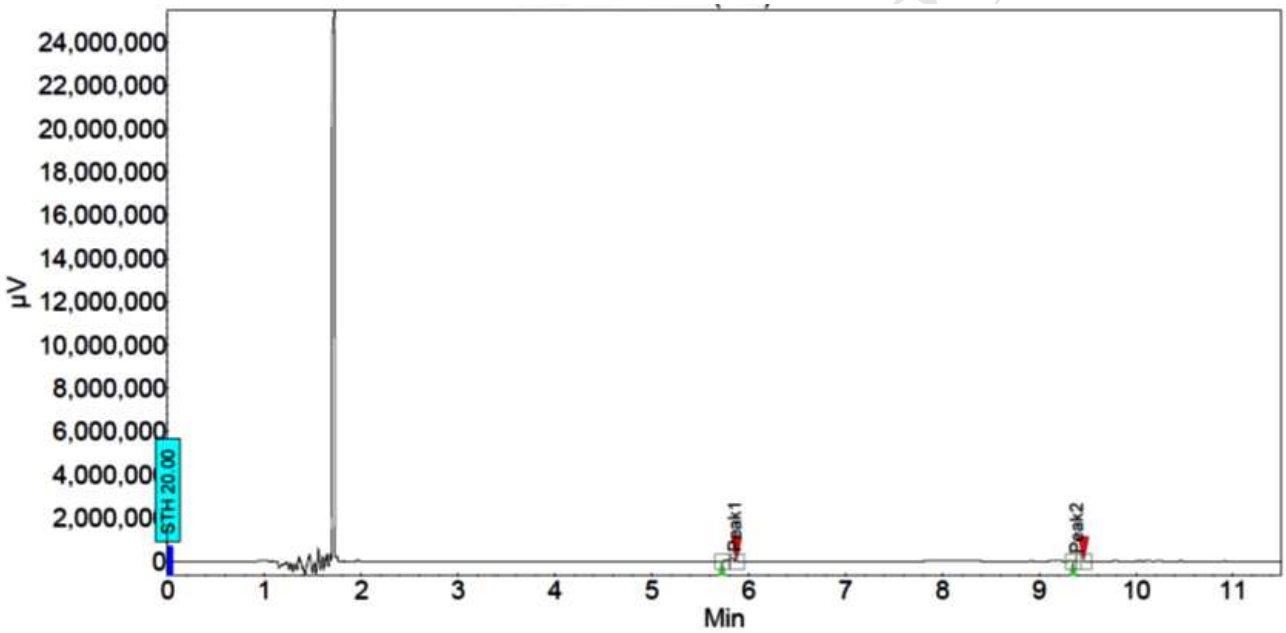

Peak results :

Index	Name	Time [Min]	Quantity [% Area]	Height [µV]	Area [µV.Min]	Area % [%]
1	Peak1	5.85	96.99	134121.2	9236.9	96.989
2	Peak2	9.38	3.01	10563.8	286.8	3.011
Total			100.00	144685.1	9523.7	100.000

Figure S14. GC Chromatogram for entry **2** in **Table 6**

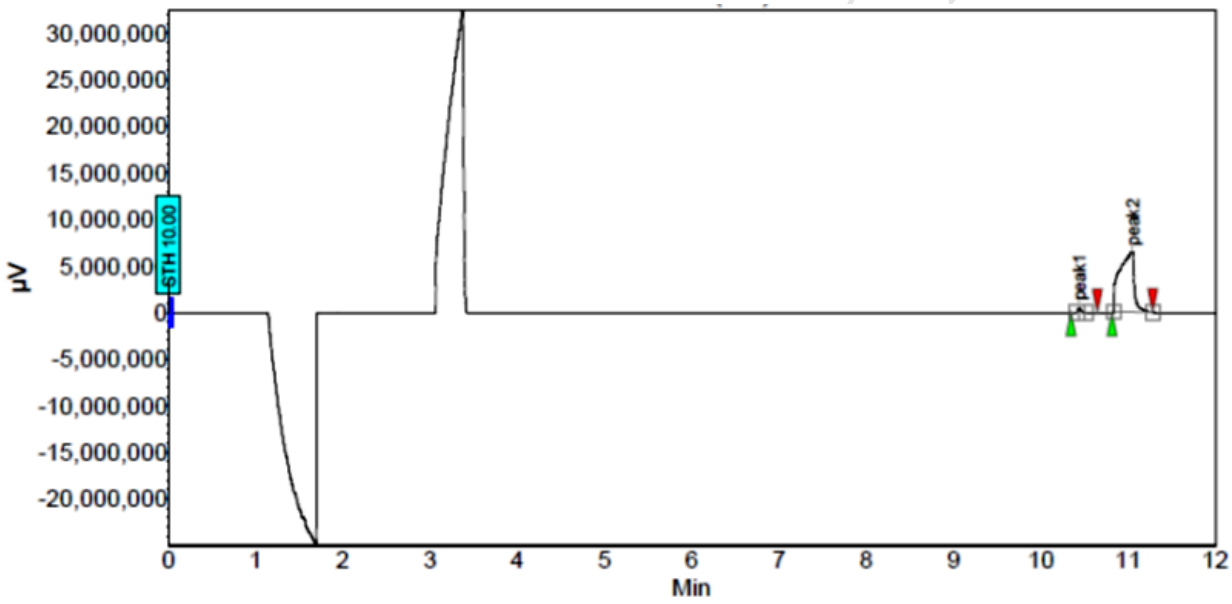

Peak results :

Index	Name	Time [Min]	Quantity [% Area]	Height [μV]	Area [μV.Min]	Area % [%]
1	peak1	10.44	1.61	595791.4	20440.5	1.613
2	peak2	11.05	98.39	6501081.6	1246756.5	98.387
Total			100.00	7096873.0	1267197.0	100.000

Figure S15. GC Chromatogram for entry **3** in **Table 6**

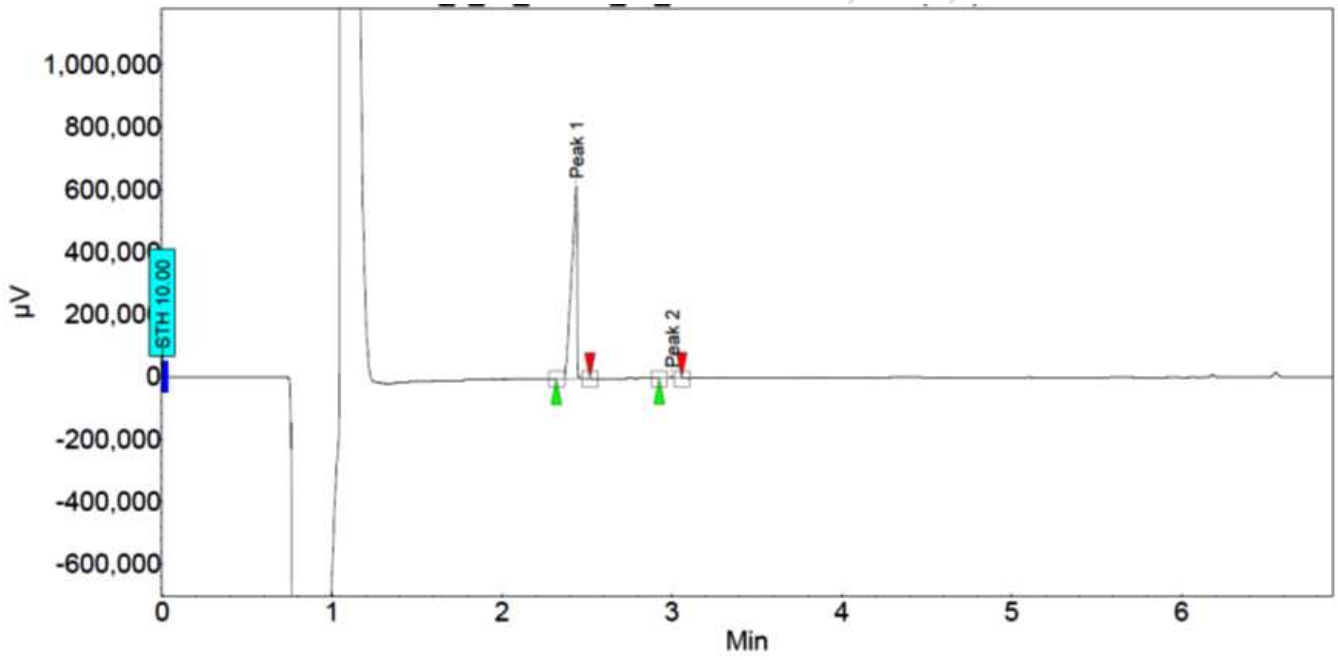

Peak results :

Index	Name	Time [Min]	Quantity [% Area]	Height [µV]	Area [µV.Min]	Area % [%]
1	Peak 1	2.44	99.25	617001.2	22965.4	99.246
2	Peak 2	3.00	0.75	5828.3	174.4	0.754
Total			100.00	622829.6	23139.8	100.000

Figure S16. GC Chromatogram for entry **4** in **Table 6**

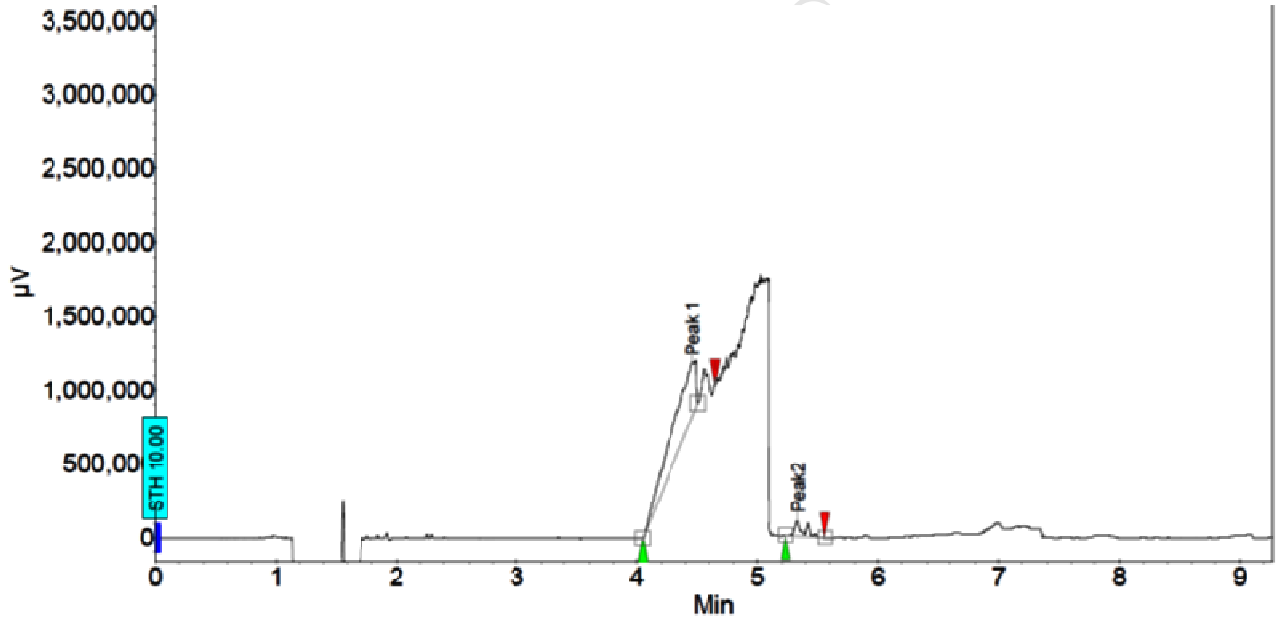

Peak results :

Index	Name	Time [Min]	Quantity [% Area]	Height [µV]	Area [µV.Min]	Area % [%]
2	Peak 1	4.45	91.03	386686.7	87716.7	91.025
1	Peak2	5.33	8.97	106624.0	8648.4	8.975
Total			100.00	473310.7	96365.1	100.000

Figure S17. GC Chromatogram for entry **5** in **Table 6**

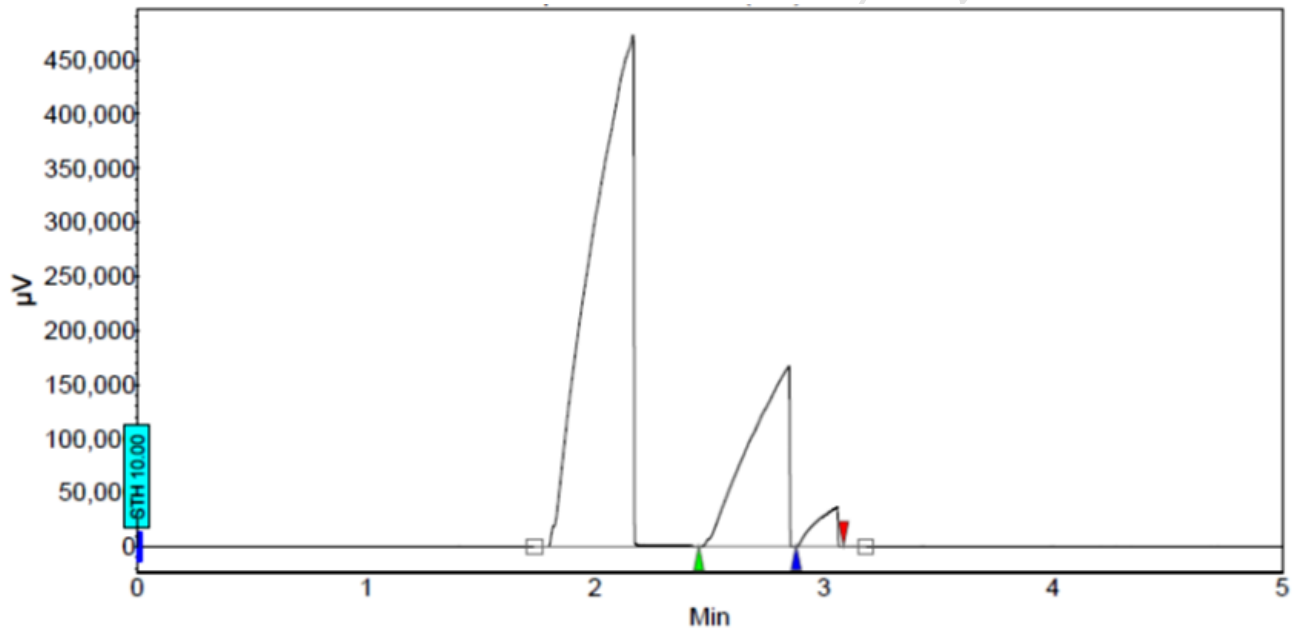

Peak results :

Index	Name	Time [Min]	Quantity [% Area]	Height [µV]	Area [µV.Min]	Area % [%]
1	UNKNOWN	2.85	89.48	166857.1	32901.4	89.476
2	UNKNOWN	3.06	10.52	35836.3	3870.0	10.524
Total			100.00	202693.3	36771.4	100.000

Figure S18. GC Chromatogram for entry **6** in **Table 6**

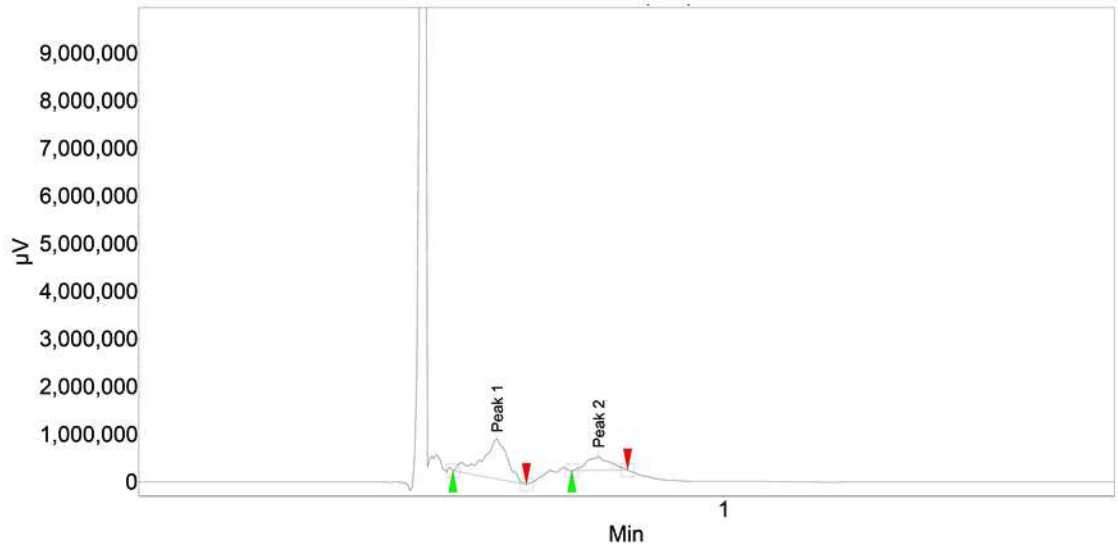

Peak results :

Index	Name	Time [Min]	Quantity [% Area]	Height [µV]	Area [µV.Min]	Area % [%]
1	Peak 1	0.83	75.52	848255.2	18601.7	75.521
2	Peak 2	0.90	24.48	311028.8	6029.3	24.479
Total			100.00	1159284.1	24631.0	100.000

Figure S19. GC Chromatogram for entry **7** in **Table 6**

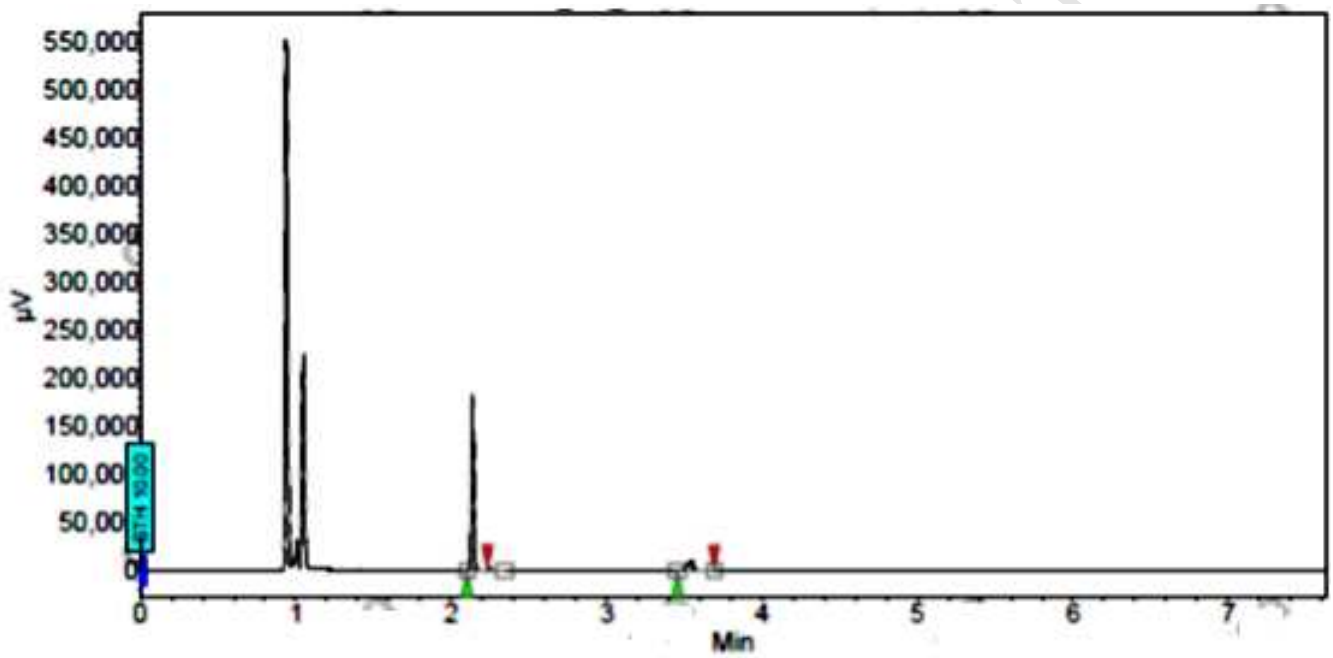

Peak results :

Index	Name	Time [Min]	Quantity [% Area]	Height [uV]	Area [uV.Min]	Area % [%]
1	UNKNOWN	2.14	84.38	181849.1	2783.4	84.377
2	UNKNOWN	3.55	15.62	10878.2	515.4	15.623
Total			100.00	192727.3	3298.8	100.000

Figure S20. GC Chromatogram for entry **8** in **Table 6**

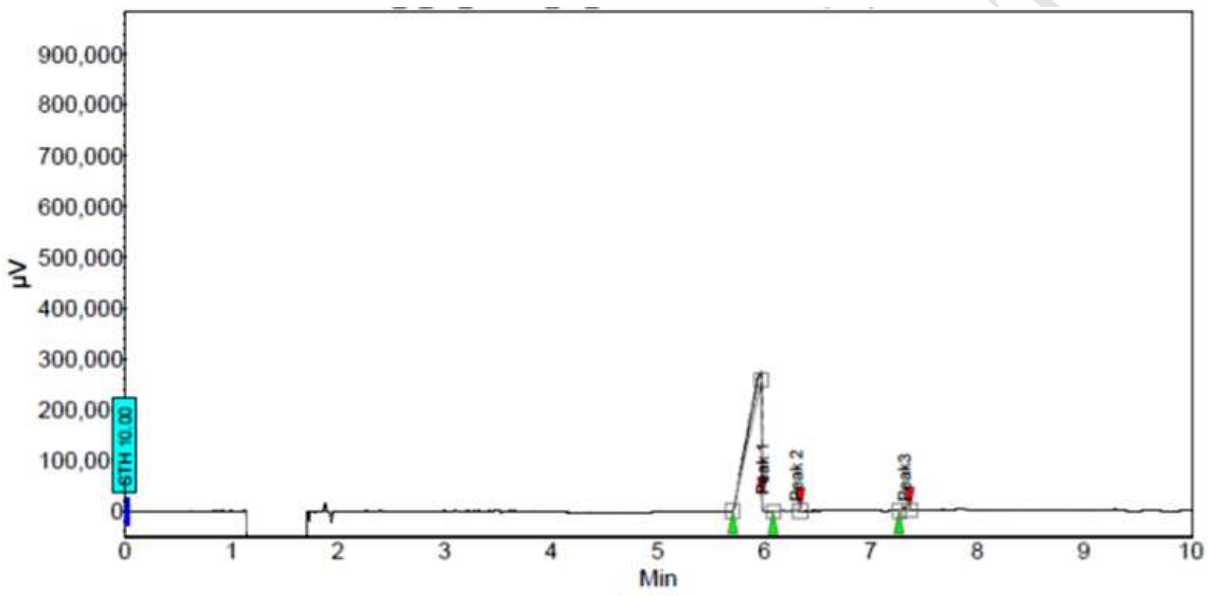

Peak results :

Index	Name	Time [Min]	Quantity [% Area]	Height [µV]	Area [µV.Min]	Area % [%]
1	Peak 1	5.98	92.61	246598.8	3860.2	92.609
2	Peak 2	6.30	2.37	1543.2	98.8	2.371
3	Peak3	7.31	5.02	5026.0	209.2	5.019
Total			100.00	253167.9	4168.3	100.000

Figure S21. GC Chromatogram for entry **9** in **Table 6**

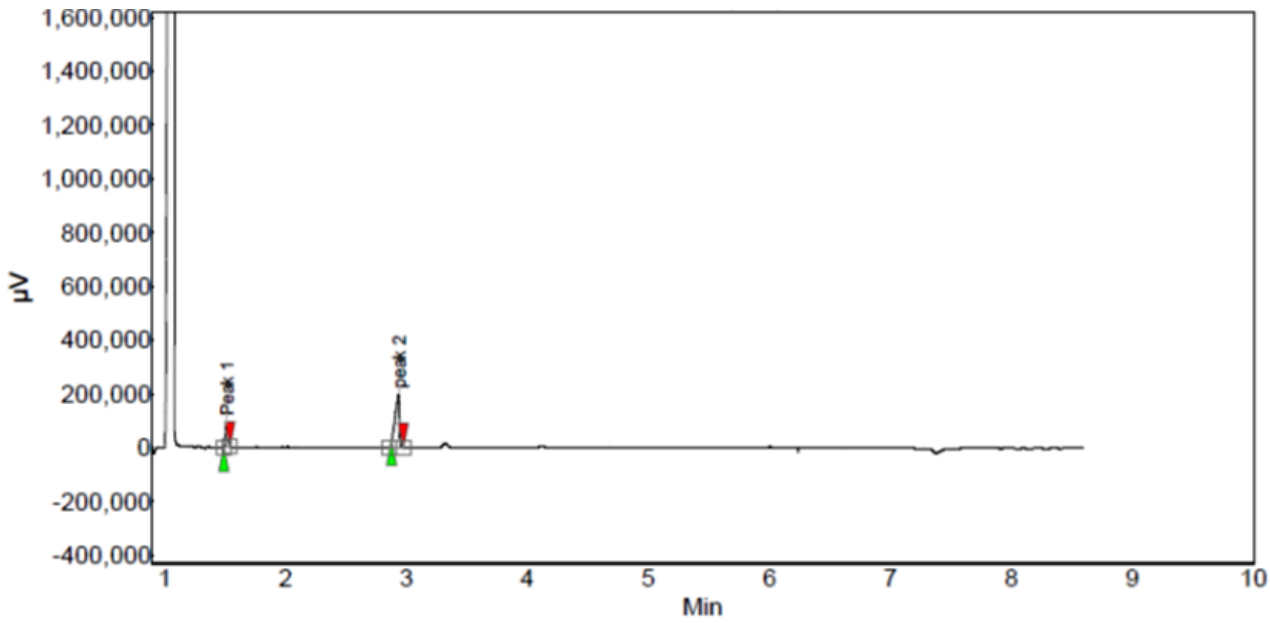

Peak results :

Index	Name	Time [Min]	Quantity [% Area]	Height [µV]	Area [µV.Min]	Area % [%]
2	Peak 1	1.51	17.51	83853.8	1725.6	17.506
1	peak 2	2.94	82.49	194707.1	8131.2	82.494
Total			100.00	278561.0	9856.8	100.000

Figure S22. GC Chromatogram for entry **10** in **Table 6**

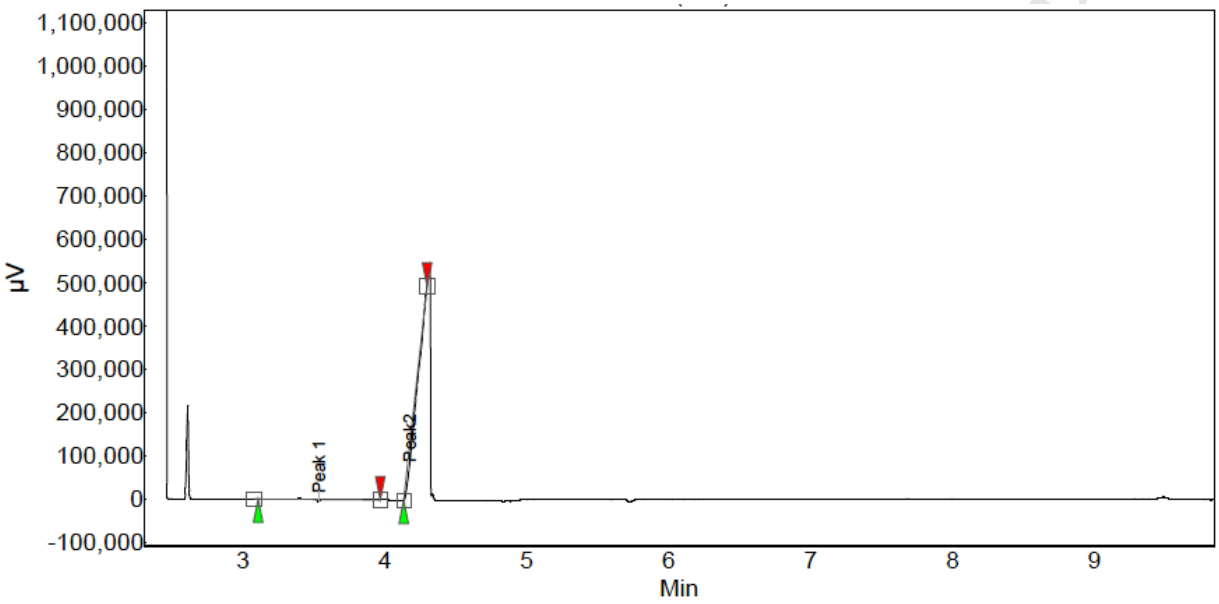

Peak results :

Index	Name	Time [Min]	Quantity [% Area]	Height [µV]	Area [µV.Min]	Area % [%]
1	Peak 1	3.53	10.69	4698.4	441.0	10.685
2	Peak2	4.17	89.31	41496.1	3686.5	89.315
Total			100.00	46194.5	4127.6	100.000

Figure S23. GC Chromatogram for entry **11** in **Table 6**

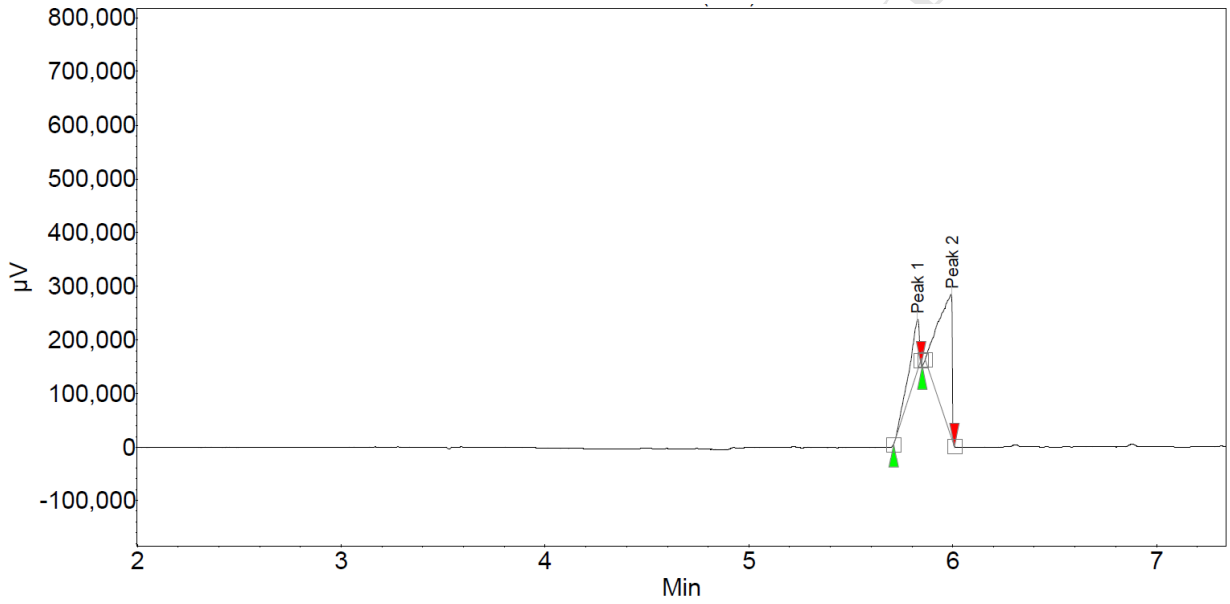

Peak results :

Index	Name	Time [Min]	Quantity [% Area]	Height [µV]	Area [µV.Min]	Area % [%]
2	Peak 1	5.83	22.06	94218.1	5387.3	22.064
1	Peak 2	5.99	77.94	264511.3	19029.7	77.936
Total			100.00	358729.4	24417.0	100.000

Figure S24. GC Chromatogram for entry **12** in **Table 6**

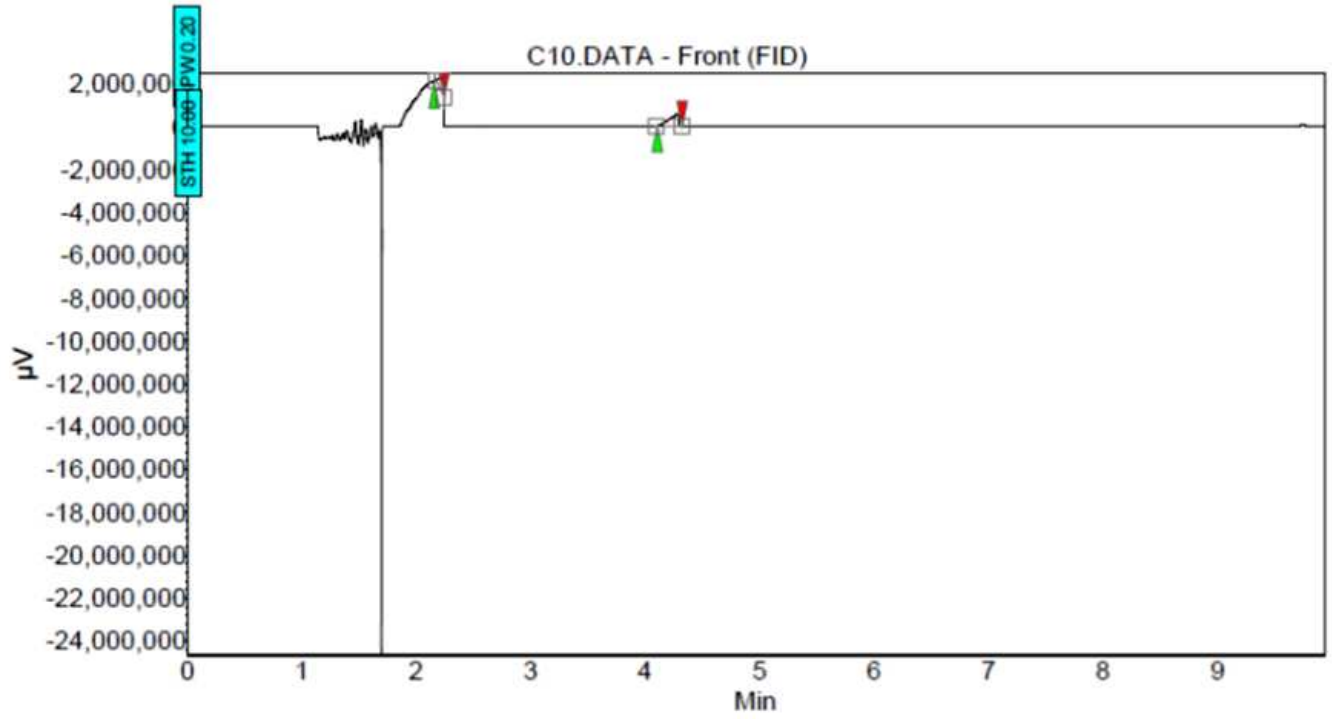

Peak results :

Index	Name	Time [Min]	Quantity [% Area]	Height [µV]	Area [µV.Min]	Area % [%]
2	UNKNOWN	2.24	34.10	1060685.9	29757.4	34.099
1	UNKNOWN	4.29	65.90	573035.5	57509.7	65.901
Total			100.00	1633721.5	87267.1	100.000

Figure S25. GC Chromatogram for entry **13** in **Table 6**

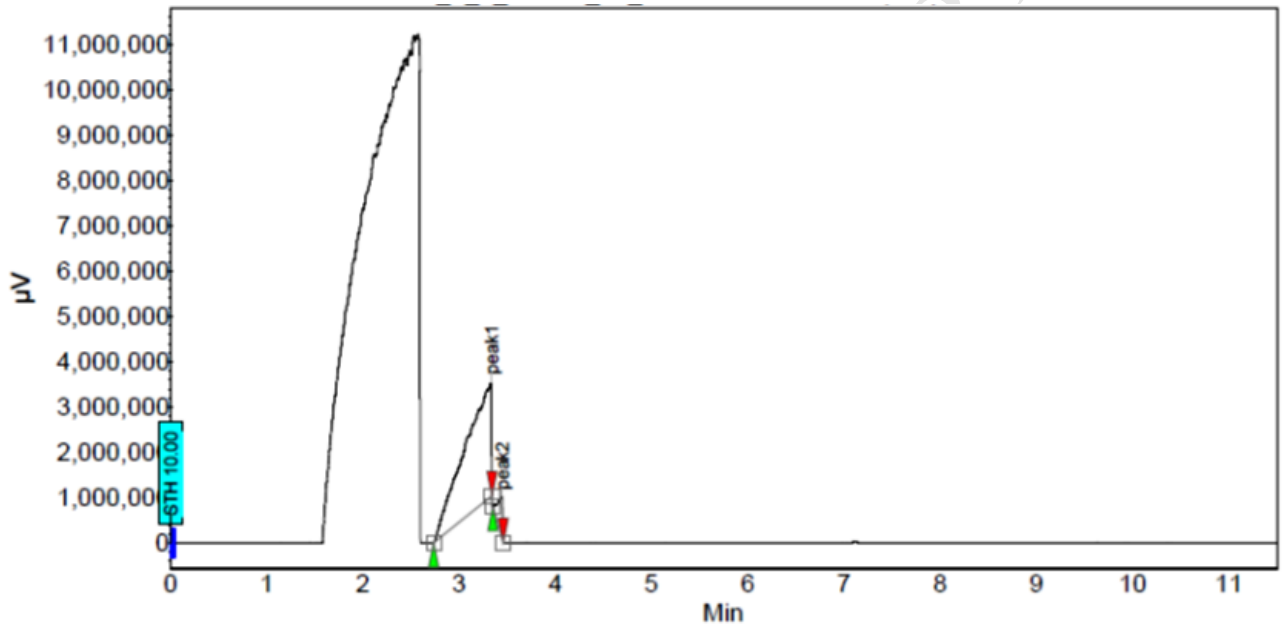

Peak results :

Index	Name	Time [Min]	Quantity [% Area]	Height [µV]	Area [µV.Min]	Area % [%]
1	peak1	3.33	94.82	2512484.8	829510.1	94.818
2	peak2	3.45	5.18	952642.8	45338.6	5.182
Total			100.00	3465127.6	874848.7	100.000

Figure S26. GC Chromatogram for entry **14** in **Table 6**

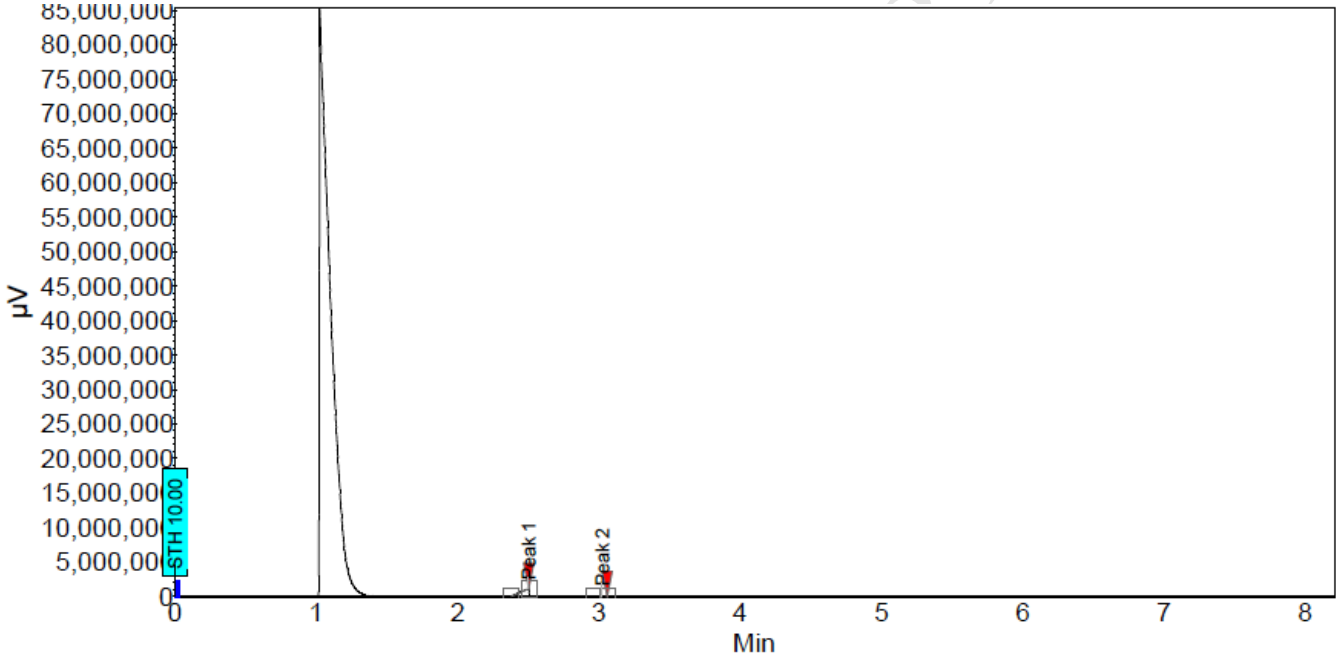

Peak results :

Index	Name	Time [Min]	Quantity [% Area]	Height [µV]	Area [µV.Min]	Area % [%]
1	Peak 1	2.50	87.76	65590.3	1827.5	87.761
2	Peak 2	3.02	12.24	10092.8	254.9	12.239
Total			100.00	75683.1	2082.4	100.000

Figure S27. GC Chromatogram for entry **15** in **Table 6**

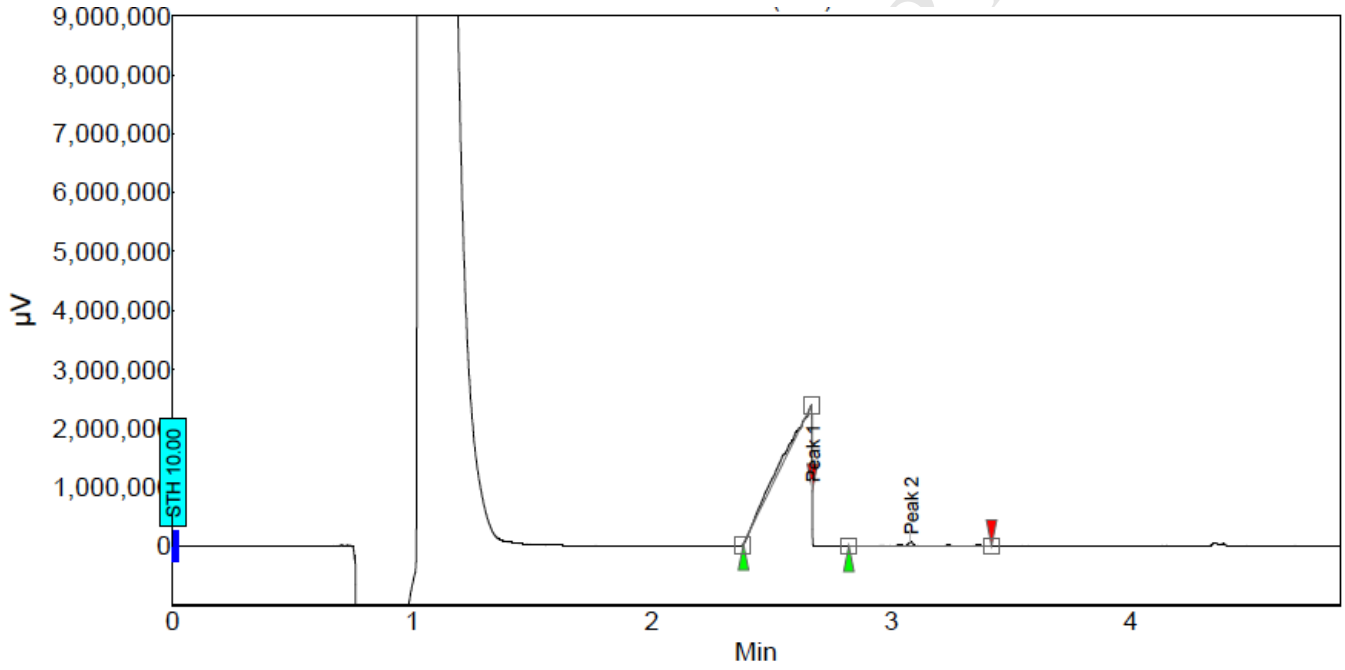

Peak results :

Index	Name	Time [Min]	Quantity [% Area]	Height [µV]	Area [µV.Min]	Area % [%]
1	Peak 1	2.67	82.56	2866976.8	13931.3	82.557
2	Peak 2	3.08	17.44	68506.7	2943.4	17.443
Total			100.00	2935483.5	16874.6	100.000

Figure S28. GC Chromatogram for entry **16** in **Table 6**